

Cyto-compatibility and anti-inflammatory effect of polyphenolic coatings on human gingival fibroblasts

Master thesis by

Mathias Reiersen and Sadaf Sarraj

Supervisors:

Hanna Tiainen and Florian Weber



Department of Biomaterials

Institute of Clinical Dentistry

University of Oslo

2022

Abstract

A rising number of patients prefer implant-retained restorations to replace missing teeth, and the majority of these implants are osseointegrated titanium implants with promising survival rates. However, inflammatory peri-implant diseases can jeopardize the long-term success of osseointegrated dental implants.

In this project, we developed a thin polyphenol-based film on the titanium (Ti) surfaces and evaluated their ability to reduce inflammation.

We examined the anti-inflammatory properties of tannic acid (TA) and pyrogallol (PG) coatings. Cytotoxicity of the formed coatings and their precursor molecules were determined with LDH assay. Pro-inflammatory cytokine release and activation of NF- κ B signaling pathway in human gingival fibroblasts cultivated on coated titanium surfaces were measured and compared to cell response on unmodified Ti surfaces and to cells exposed to dissolved TA and PG molecules.

By building on this knowledge, we hope to contribute to the development of therapeutically practical infection-resistant polyphenol-coated implant surfaces that may modify the wound healing response elicited by the host tissue upon implant insertion.

Acknowledgements

We would like to thank everyone at the Department of Biomaterials, at the Institute of Clinical Dentistry, University of Oslo, for their support and generosity. We could not have done it without your supportive comments and willingness to help, from the slightest of questions to the most difficult of duties.

First and foremost, we want to express our gratitude to Hanna Tiainen and Florian Weber, our supervisors, for their unconditional support, inspiration, and encouragement.

In addition, we would like to express our gratitude to Aina-Mari Lian and Catherine Anne Heyward for their assistance during our research.

Above all, we want to thank our family and friends for their unwavering support throughout the thesis process.

We are sincerely grateful to the faculty for granting us a summer fellowship for student research in 2020, which allowed us to complete the essential laboratory work for our master thesis.

Table of content

Abstract	1
Acknowledgements	2
Table of content	3
Abbreviations and notations.....	4
1 Introduction.....	5
1.1 Dental implants.....	5
1.2 Host tissue integration and peri-implant wound healing	6
1.3 Inflammation process	8
1.4 Peri-implantitis	9
1.5 Strategies to improve host tissue integration	10
2 Materials and methods	13
2.1 Sample preparation and coating formation.....	13
2.2 Coating properties	13
2.3 Cell culture	13
2.4 Cytotoxicity.....	14
2.5 Inflammatory response	14
2.6 Cell morphology.....	15
2.7 Statistical analysis	15
3 Results and discussion	16
3.1 Coating formation.....	16
3.2 Deposition kinetics of tannic acid at pH 6.8 (TA6.8).....	17
3.3 Deposition kinetics of tannic acid at pH 7.8 (TA7.8).....	18
3.4 Deposition kinetics of pyrogallol at pH 7.0.....	20
3.5 Cytotoxicity	22
3.6 Inflammatory markers	24
3.7 NF- κ B activation	26
3.8 Cell morphology.....	27
4 Conclusions.....	28
5 References	29
6 Appendix.....	37

Abbreviations and notations

C-	negative control
C+	positive control
DAPI	4',6-diamidino-2-phenylindole
hGF	human gingival fibroblast
IL	interleukin
LDH	lactate dehydrogenase
LPS	lipopolysaccharide
MCP-1	monocyte chemoattractant protein-1
NF- κ B	nuclear factor kappa B
NF- κ B p65	nuclear factor kappa B p65, also known as RelA
PG	pyrogallol / titanium surface coated with pyrogallol at pH 7.0
QCM-D	quartz crystal microbalance with dissipation monitoring
ROS	reactive oxygen species
TA	tannic acid / titanium surface coated with tannic acid at pH 6.8
TA _{ox}	titanium surface coated with tannic acid at pH 7.8
TCP	tissue culture plastic
Ti	uncoated titanium surface
TNF- α	tumor necrosis factor alpha

1 Introduction

Tooth loss can have a substantial impact on one's quality of life (Gerritsen, Allen, Witter, Bronkhorst, & Creugers, 2010). Patients that are missing teeth often experience loss of phonetic function, eating difficulties and social humiliation (Allen, 2003). Loss of a tooth can be caused by trauma, dental infections such as caries or periodontitis, or as a result of cancer treatment. Oral infections impact over 3.5 billion people globally, making it one of the most frequent public health challenges (Vos et al., 2017).

Severe periodontal disease affects roughly 10% of the European population (Aubrey & Gopalakrishnan, 2002). Traditionally dental bridges have been used to replace missing teeth and restore aesthetic, masticatory, and phonetic function. Because of the excellent success rate of 95%, dental implants have grown more popular in recent years (Moraschini, Poubel, Ferreira, & dos Sp Barboza, 2015). In the years 2014 to 2017, 15 000 dental implants were inserted in Norway alone (Lie et al., 2019).

1.1 Dental implants

Implants come in a multitude of shape and sizes, and they are made by a variety of companies. Despite variations in the design of the implant, a basic buildup is universal. Endosseous implants are made up of three parts: an implant body, an abutment, and a crown (Figure 1). The body of the implant is fixed to the jawbone and serves as a stable foundation for the crown. The abutment connects the crown to the implant.

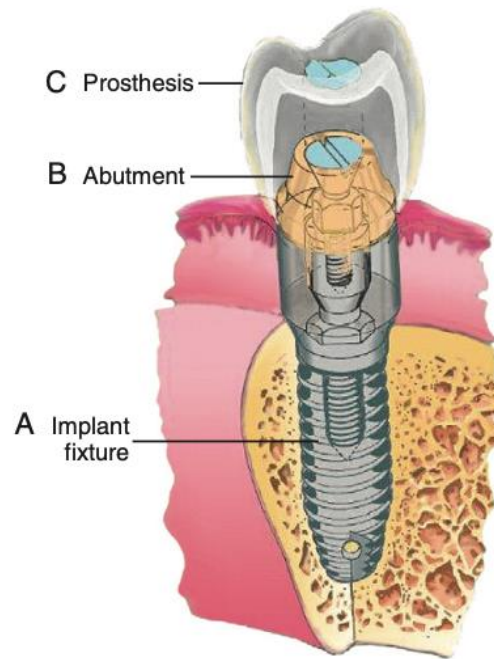


Figure 1: Diagram of implant components: A) the implant fixture (endosteal root form), B) transmucosal abutment serving as the attachment between fixture and the actual prosthesis, C) the actual prosthesis (crown), which can either be cemented, screwed, or swaged (Anusavice, Shen, & Rawls, 2012).

For its high mechanical qualities and corrosion resistance, titanium has become a popular biocompatible implant material (Van Noort, 1987). In comparison to noble metals such as gold, titanium and its alloys provides sufficient mechanical strength and are less brittle than ceramics (Osman & Swain, 2015). In contact with either water or air, a stable oxide layer is formed, which is responsible for the remarkable biocompatibility of titanium (Donachie, 2000). In addition, this layer is responsible for corrosion resistance and reduced ion leakage into the surrounding tissue (Williams, 1976). The lack of periodontal ligament allows for physical contact between titanium and bone, which is essential for the function of dental implant insertion (Adell, Lekholm, Rockler, & Brånemark, 1981). This characteristic is defined as osseointegration (Bosshardt, Chappuis, & Buser, 2017).

1.2 Host tissue integration and peri-implant wound healing

As soon as the implant is inserted into the jaw, a foreign body reaction takes place. The host's response to foreign objects affects the process of wound healing, and the final tissue integration of the implant. Generally, the process is divided into three phases. Firstly, the body responds with inflammation to the surgical trauma and implant surface. Secondly, there is a regeneration, where there is the formation of new soft and hard tissues, and lastly a remodeling stage (Byrne, 2014). In

the remodeling phase the fibroblasts remodel granular tissue, and seal the gingiva to protect the implant from the oral cavity (Bainbridge, 2013).

At the site of tissue damage and contact with blood, the coagulation and complement system is activated. The complement system is a part of the innate immune system and is critical in the defense mechanism against pathogens (Merle, Church, Fremeaux-Bacchi, & Roumenina, 2015). By recognizing the implant as foreign, the complement system triggers phagocytic cells, such as neutrophils, monocytes, and macrophages to eliminate it (Merle, Noe, Halbwachs-Mecarelli, Fremeaux-Bacchi, & Roumenina, 2015). As the coagulation system is activated, the wound healing process begins as well. A blood clot, composed of components of extracellular matrix and platelets inhibits bleeding. The extrinsic and intrinsic coagulation pathways are triggered by tissue injury and the implant surface. Both pathways generate tissue factors (TFs).

Thrombin levels increase when the coagulation is activated, causing fibrinogen to become fibrin (Antoniak, 2018). Through the action of coagulation factors, such as thrombin, platelets are then activated, which leads to increased production of thrombin (Heemskerk, Bevers, & Lindhout, 2002). A clot of fibrin meshes and entrapped platelets are formed as a result. Thrombin will stimulate the production of pro-inflammatory cytokines, and therefore coagulation is important in the inflammation. In addition, continuous activation of platelets and persistent inflammation tend to reduce fibrinolysis. As the acute inflammatory phase ends, the regeneration phase begins. Various processes take place during this stage. Cells such as leukocytes and fibroblasts respond to cytokines and growth factors around the wound. And the extracellular matrix (ECM) is formed by fibroblasts proliferation (Barrientos, Stojadinovic, Golinko, Brem, & Tomic-Canic, 2008). The ECM is modified throughout the regeneration phase.

Hard tissue develops because of osteogenic and angiogenic processes. Osteoprogenitor cells from the bone marrow move to the site of the wound, where they multiply and distinguish into osteoblasts. These cells begin to form hard tissue on the surface of the surrounding bone and the surface of the implant (Lang, 2019). Adaptation to the surroundings is a continuous process that needs ongoing rebuilding (Lang, 2019). Within a few days, the acute inflammation will be reduced, and the healing mechanism will take control. The implant has intimate contact with the surrounding hard tissue, after a few months. The implant is now osseointegrated, and its survival rate is roughly 95% at this time (Moraschini et al., 2015).

In addition to osseointegration, an adequate integration of soft tissue on the coronal implant surface is critical for implant longevity because it offers protection against microbial infection (Zhao et al.,

2014). Nevertheless, chronic wounds or patients with impaired wound healing should be treated as soon as possible. As result of the infection, acute inflammation is prolonged, and the healing is disrupted. Consequently, bacterial contamination can invade the area of the implant, and lead to infection of the implant, such as mucositis and peri-implantitis. The consequence of this will be bone resorption, which leads to failure of the implant (Weber, 2021).

1.3 Inflammation process

Inflammation is a natural process that is part of the innate immune response to foreign objects, such as bacteria or implants. Firstly, local leukocytes recognize a stimulus with specific cell surface pattern receptors, this activates intracellular inflammatory pathways. Inflammatory markers are released and inflammatory cells are recruited (L. Chen et al., 2018). Foreign objects work here as the stimuli and activate the complement system which in turn leads to recruitment of circulating leukocytes to the area (Merle, Church, et al., 2015). Macrophages and neutrophils are considered as some of the most important leukocytes of the innate immune system as they can express various inflammatory cytokines and eliminate foreign objects by phagocytosis. This is done by releasing reactive oxygen species (ROS), which cause local acidosis, damaging all surrounding cells without discrimination (Serhan, Ward, & Gilroy, 2010). Activated macrophages again express pro-inflammatory cytokines which attract more leukocytes and trigger inflammation in the surrounding tissue (Johnson, 1997).

Cytokines such as IL-6, IL-8 and MCP-1 and TNF- α are important in cell communication and in inducing inflammation (Figure 2). Using different pathways, the aforementioned cytokines are recognized by cytokine specific receptor complexes on cell surfaces and the signal cascades activate gene expression in the cell nucleus. Activation of NF- κ B in the nucleus upregulates a multitude of genes that are involved in fundamental physiological and pathophysiological cellular processes such as activation of the immune system, especially of the innate immune system, as well as the regulation of inflammation and apoptosis (Neumann & Naumann, 2007). The same inflammation response may be triggered by bacterial and fungal lipopolysaccharides (LPS) (Pålsson-McDermott & O'Neill, 2004). Cytokines such as IL-10 and TGF- β are important in inhibiting the inflammation process. In similar pathways, the cytokines regulate the immune system by limiting the inflammatory response that could lead to tissue damage (Sanjabi, Zenewicz, Kamanaka, & Flavell, 2009).

Regarding tackling inflammation, we can therefore regulate the process at different stages. The inhibition of inflammation reduces ROS and the tissue destructive processes which are essential in wound healing. A theory tested in this thesis is that an already ongoing inflammation process with

present pro-inflammatory cytokines can still be prevented by blocking intracellular signaling pathways. This process, however, needs to be highly regulated as suppressing the immune response can potentially lead to uncontrolled microbial growth.

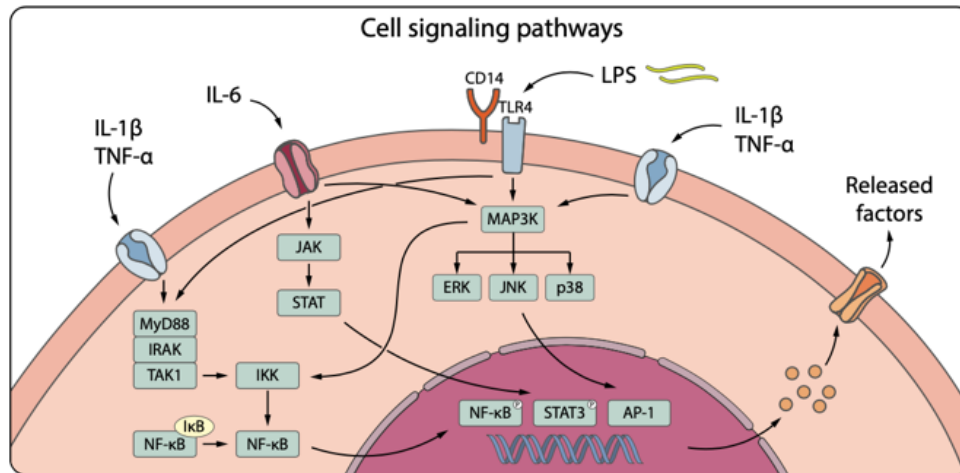


Figure 2: Different cytokines and inflammatory substances enter the cell membrane through specific receptors. They stimulate multiple intracellular mechanism which ultimately leads to the production and release of inflammatory factors initiating and maintaining inflammation (Weber, 2021).

1.4 Peri-implantitis

The oral cavity is always full of bacteria that can adhere to the implant surface and cause infection and inflammation. These inflammatory lesions affecting the tissue surrounding the dental implant are known as peri-implant disease (Zitzmann & Berglundh, 2008). This can either be peri-implant mucositis or peri-implantitis, defined as the destructive inflammatory process caused by bacteria that affect the soft and hard tissues around osseointegrated implants, respectively (Mombelli, Müller, & Cionca, 2012).

Peri-implant mucositis is the reversible soft tissue inflammation around a functioning implant which is seen before the development of peri-implantitis. The disease firstly becomes irreversible when there is a pathological condition in the peri-implant connective tissue, and we see progressive loss of supporting bone (Schwarz, Derks, Monje, & Wang, 2018). Without proper treatment of peri-implantitis the implant will have continued loss of osseointegration which can eventually lead to implant failure (Bodet, Chandad, & Grenier, 2007).

Delving into the literature we can put the prevalence of peri-implantitis between 10% to 30%, but in some studies, it can exceed 70% depending on the assessment criteria (Krebs et al., 2019). Patients with pre-existing diseases or habits that affect wound healing, e.g. diabetes, smoking and auto-

immune diseases, are at a higher risk of developing peri-implant diseases (Turri, Orlando Rossetti, Canullo, Grusovin, & Dahlin, 2016). Bacterial complexes typically associated with periodontal disease are also found on the surface of implants affected with peri-implantitis (Perez-Chaparro et al., 2014). It is therefore discussed that patients with periodontal disease are at a higher risk of developing peri-implantitis (Polizzi et al., 2000). Another important aspect is the implant design and implant surface. Increased biofilm accumulation has been observed on especially rough surfaces (Cosyn, Sabzevar, De Wilde, & De Rouck, 2007). This most likely has to do with adhesion of bacteria in the micro roughness on the implant surface and the increased difficulty keeping the surface clean during oral hygiene measures (Esposito, Hirsch, Lekholm, & Thomsen, 1997). Because of this, most implants used today are polished on the surfaces that are exposed to soft tissue. Either way, where peri-implantitis is present, the progressive bone loss eventually exposes the rougher cervical implant surfaces, and the implant becomes difficult to keep adequately clean (Mombelli, 2002).

Treatment of peri-implantitis consists of mechanical debridement of the implant surface, such as debridement with Ti-curettes, with or without the use of chemical disinfectants or antibiotics (Javed et al., 2013). However, there is evidence that on the exposed rough surfaces, the usage of antimicrobial agents has limited effect (Carcuac et al., 2016). Another treatment is implantoplasty, which is not an optimal treatment as the implant will be weakened after implantoplasty (Camps-Font et al., 2020).

We need new ways to fight peri-implant diseases and find an implant that is both antimicrobial and easily osseointegrated while also being of the desired mechanical strength. We therefore try to change the surface chemistry of dental implants with the aim to prevent the initial colonization by bacteria and enhancing soft tissue attachment to work as a barrier against the critical stage of initial microbial invasion.

1.5 Strategies to improve host tissue integration

When an implant is inserted, the surface of the implant will be introduced to the host tissue initially. As a result, the implant surface has a significant impact on how the tissue will react to the foreign substance.

The implant-tissue interaction can be affected and modified by surface properties, including both physical and chemical features (Boyan, Hummert, Dean, & Schwartz, 1996). Studies have shown that increased contact area and retention can be achieved with a rough surface on the implant (Abrahamsson, Berglundh, Linder, Lang, & Lindhe, 2004). Simultaneously, it also encourages bone growth (Elias & Meirelles, 2010). Therefore, nearly all modern implant systems have been altered to

improve surface roughness. Surfaces that come into touch with soft tissue, on the other hand, are typically smooth to prevent bacterial infiltration.

In addition to the physical features, the chemical properties can also affect the interaction between the implant and the soft tissue. It can affect the protein adsorption and cell adhesion (Boyan et al., 1996). Therefore, the development of creating implant surfaces able to cope with challenging conditions of reduced host systems and bacterial infection has been of interest. Extracellular matrix proteins, growth factors, short peptides, and antibacterial compounds are all potential substrates for biochemical coatings (X. Chen, Li, & Aparicio, 2013).

The inadequate biocompatibility of most antibacterial surfaces and growth factor stability after insertion of an implant are the major reason for the current implant market's lack of such products (Gruber & Bosshardt, 2015). The antibacterial strategies are primarily intended to prevent the colonization of bacteria on the implant surface (Campoccia, Montanaro, & Arciola, 2013).

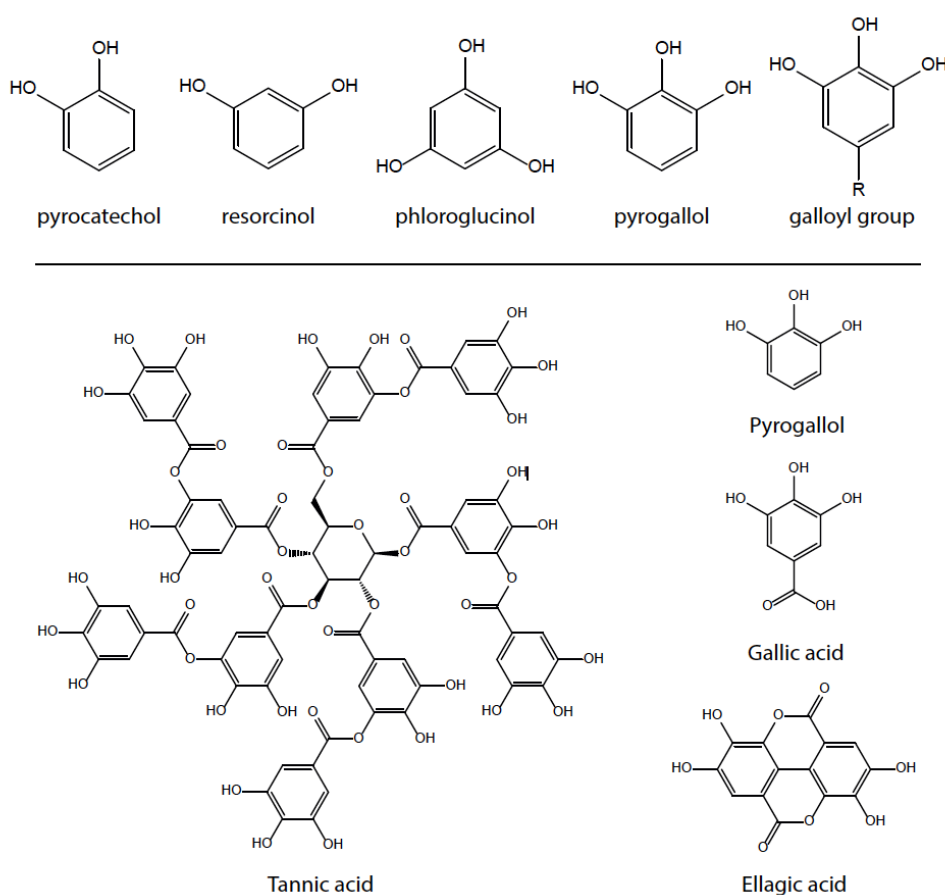


Figure 3: Polyphenols are a group of naturally occurring organic molecules consisting of one or more benzene rings with at least two hydroxyl groups attached to the aromatic ring of the molecule. Tannic acid represents a complex hydrolysable polyphenol consisting of several pyrogallol and galloyl groups. Hydrolytic degradation of tannic acid in aqueous environments, such as physiological fluids, typically yield tannic acid and ellagic acid. (Weber, 2021)

Polyphenols have recently been of interest to create coatings on the implant surface. Polyphenols are compounds of benzene consisting of several hydroxyl groups (Figure 3). Changes in the quantity and arrangement of the hydroxyl groups allow the polyphenols to have a wide range of properties. These molecules are normally found in plant tissues, where they perform a variety of biological roles, such as growth, antimicrobial, anti-inflammatory, and antioxidant properties (Quideau, Deffieux, Douat-Casassus, & Pouységu, 2011). These properties make polyphenols a particularly interesting group of biomolecules with remarkable potential to decrease inflammation and infection in peri-implant tissues. For example, polyphenols such as proanthocyanidins, flavonoids and tannins obtained from red cranberries and tea have been found to influence bacterial virulence and host response to periodontal pathogens. They might be used to treat periodontal disease, because of their ability to suppress periodontal pathogens and inflammation associated with periodontal disease (Feghali, Feldman, La, Santos, & Grenier, 2012), (Palaska, Papathanasiou, & Theoharides, 2013).

Because of these apparent antioxidant and anti-inflammatory properties of plant polyphenols, we have chosen to look deeper into the effect of the polyphenols tannic acid (TA) and pyrogallol (PG), as well as coatings consisting of these polyphenols, on cell viability and anti-inflammatory potential in human gingival fibroblasts. These molecules were chosen for their ability to form nanocoatings on titanium surface (Barrett, Sileika, & Messersmith, 2014), (Geißler, Barrantes, Tengvall, Messersmith, & Tiainen, 2016), and the high antioxidant, and thereby, high anti-inflammatory potential associated with the pyrogallol structure that features in both molecules (Jang, Hyam, Jeong, Han, & Kim, 2013), (Rahman, Biswas, & Kirkham, 2006), (Zhan, Ejima, & Yoshie, 2016).

2 Materials and methods

2.1 Sample preparation and coating formation

Grade IV titanium disks ($\emptyset 6 \times 3$ mm) were mirror-polished and washed as described previously and autoclaved for 20 min at 121°C. The disks were then aseptically coated in vials containing 10 ml of 1 mg/ml polyphenol solution on a rocking platform at 30 rpm for 24 h. Tannic acid solution contained 100 mM HEPES, 600 mM NaCl, 100 μ M sodium metasilicate at either pH 6.8 (TA) or pH 7.8 (TA_{ox}). Pyrogallol solutions contained 100 mM HEPES, 100 mM MgCl₂ at pH 7.0. After the coating formation, disks were washed and sonicated in sterile water to remove unbound molecules and precipitated particles. The coated surfaces are referred to as TA, TA_{ox} and PG, while the uncoated polished titanium surfaces used as control are referred to as Ti. All chemicals used for the coating formation were purchased from Sigma Aldrich.

2.2 Coating properties

The coating formation on titanium surface was investigated in real time by means of a QCM-D system (Q-Sense E4, Biolin Scientific, Sweden). TA, TA_{ox} and PG coatings were deposited on titanium coated quartz crystals (QXS 310, Biolin Scientific, Sweden) using a flow system described previously (Geißler et al., 2016). Briefly, the coating solutions were stirred at 100 rpm outside the instrument while being pumped over the quartz crystal at room temperature using a flow rate of 100 μ l/min. During coating deposition, changes in resonance frequency (Δf) and dissipation factor (ΔD) were constantly monitored. The obtained data of the third, fifth, and seventh overtones are presented in two different ways: either versus time (Δf -t and ΔD -t plots) or as ΔD versus Δf (ΔD - Δf plots). In addition, QTools software (Biolin Scientific, Sweden) was used to obtain information about coating thickness using the Sauerbrey model.

2.3 Cell culture

Human gingival fibroblasts (hGF; Provitro) were routinely cultured at 37°C/5% CO₂ in Dulbecco's modified Eagle's medium (DMEM), containing 4500 mg/ml glucose, 10% fetal bovine serum (FBS), 50 U/ml penicillin, 50 mg/ml streptomycin, and 2 mM GlutaMAX. Cells were subcultured before reaching confluence using trypsin/EDTA. Trypan blue stain was used to determine total and viable cell number. Cells were seeded at a density of 7×10^3 cells/well in 96-well plates. Experiments were performed with cells at passages ≤ 8 after isolation.

2.4 Cytotoxicity

Cells seeded on 96-well plates were exposed either to polyphenol-coated titanium disks or to polyphenolic molecules dissolved in cell culture medium at concentrations ranging from 1 to 500 µg/ml to assess the cytotoxicity of the polyphenolic coating and their precursor molecules on hGFs. Lactate dehydrogenase (LDH) activity was measured as an indicator for membrane related cell death. 100 µl of cell culture medium was collected after 24 h and mixed 1:1 with a reaction mixture according to manufacturer instructions (Cytotoxicity detection kit, Roche Diagnostics, Mannheim, Germany), and incubated at RT for 30 min. The oxidation of NADH was measured spectrophotometrically (ELx800, BioTek Instruments, VT, USA) at 490 nm. Results for test groups are given relative to a low control (cells on tissue culture plastic) and a high control (cells on tissue culture plastic with 1% Triton X-100) according to the following equation:

$$\text{Cytotoxicity (\%)} = \frac{\text{sample} - \text{low control}}{\text{high control} - \text{low control}} \times 100$$

Phase contrast microscopy was used to assess the morphology of the cells cultured in the presence of dissolved polyphenolic molecules following 24 h incubation at 37°C/5% CO₂.

2.5 Inflammatory response

Following 2 h incubation at 37°C/5% CO₂ to allow cell adhesion on the surface of the sample disks, cell culture medium was removed from the wells and the cells were washed gently with phosphate-buffered saline (PBS). Inflammation was then induced by incubating the cells in serum depleted medium (1% FBS) containing 1 µg/ml *Porphyromonas gingivalis* derived lipopolysaccharide (LPS) and 1 ng/ml IL-1β for up to 48 hours at 37°C/5% CO₂. These supplements were always added freshly before medium change throughout the experiments. We used a positive control of pure tissue-culture polystyrene (C+) and a negative control of tissue-culture polystyrene without LPS and IL-1β stimulation (C-).

Multianalyte profiling was performed to measure inflammatory markers secreted in cell culture medium from hGFs after 6, 24, and 48 h induced inflammation using the Luminex 200 system (Luminex, Austin, TX, USA). Median fluorescent intensity was analyzed using a 5-parameter logistic line-curve fitting method for calculating analyte concentrations in samples via the xPONENT 3.1 software (Luminex). Levels of interleukin-6 (IL-6), interleukin-8 (IL-8), monocyte chemoattractant protein-1 (MCP-1), and tumour necrosis factor-alpha (TNFα) were measured using Human

Cytokine/Chemokine Magnetic Bead Panel kit (EMD Millipore, Billerica, MA, USA). The assay was performed according to the protocol provided by the manufacturer.

Total and phosphorylated (pS536) NF- κ B p65 levels in hGFs were determined 2, 6, and 24 h after induced inflammation using the respective Human InstantOne™ ELISA kits (Invitrogen, Thermo Scientific, Waltham, MA, USA) according to the protocol provided by the manufacturer.

2.6 Cell morphology

To assess cell morphology following induced inflammation for 48 h, the cells were carefully washed with PBS and fixed with 4% paraformaldehyde for 20 min at RT. Cells were stained with 0.5 U/ml Alexa Fluor 568 Phalloidin and 300 nM DAPI dissolved in PBS containing 0.2% Triton X-100 for 30 min at RT in the dark. Three non-overlapping images were taken on two samples of each group using a Leica SP8 upright confocal laser scanning microscope (CLSM) with a 10 \times /0.40 HCPL APO CS objective.

2.7 Statistical analysis

The inflammatory response between the different groups was compared using one-way analysis of variance (ANOVA) in SigmaPlot 14.0 (Systat Software, San José, CA, USA). Pairwise multiple comparisons were performed using the Holm-Sidak method. Values are presented as mean \pm standard deviation. Statistical significance was considered at $p < 0.05$.

3 Results and discussion

3.1 Coating formation

PG and TA nanocoatings were produced on titanium surfaces by dipping the substrates in the coating solutions while being on a rocking platform as reported by Sileika et al (Sileika, Barrett, Zhang, Lau, & Messersmith, 2013). The uncoated Ti coin showed a clean polished surface. As the titanium coins were exposed to the polyphenolic solutions for 24 h and were rinsed carefully with water, we could clearly see a change in the surface of the coated coins (Figure 4). TA showed a homogenous surface coating with the color of yellow. Both TA_{ox} and PG had different areas where the coating was slightly different resulting a color pattern, having colors from purple to copper.

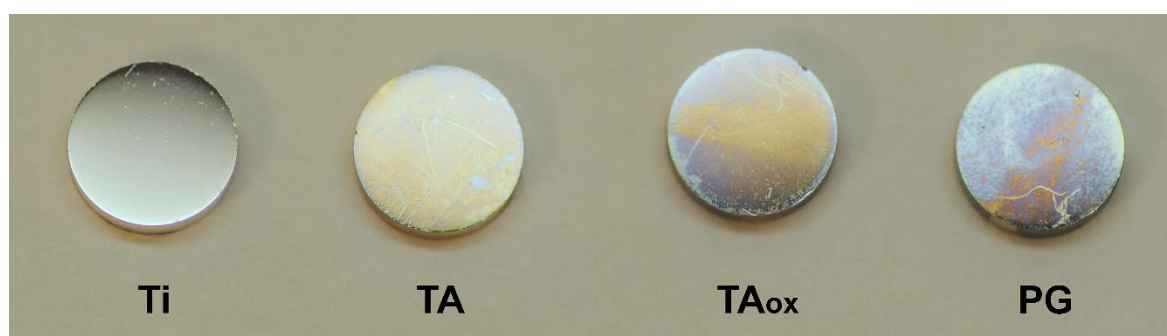


Figure 4: Polyphenolic nanocoatings formed on polished titanium disks. Ti: polished titanium disk before coating (control), TA: titanium disk with tannic acid coating formed at pH 6.8, TA_{ox}: titanium disk with tannic acid coating formed at pH 7.8, PG: titanium disk with pyrogallol coating formed at pH 7.0.

Studying the coating deposition on titanium surface in more detail requires instrumentation with high sensitivity to register the adsorption process down to the molecular level. Therefore, quartz crystal microbalance with dissipation monitoring (QCM-D) was used to investigate coating formation on titanium surface further and to determine the thickness of the deposited TA and PG nanocoatings. This method applies acoustic waves to detect mass change following molecular adsorption on a piezoelectric sensor, allowing the adsorption kinetics and adsorbed film thickness to be calculated (Johannsmann, 2015). Compared to other methods, QCM-D has the ability and advantage to gather information also about the structural properties of the deposited thin film in real time (Höök et al., 2002). The agitation of the rocking platform was in this case mimicked by stirring the polyphenolic solutions outside the system and ensuring sufficient oxygen that is required for the oxidation reaction (Geißler et al., 2016). The deposition kinetics of polyphenolic solutions on titanium-coated quartz crystals was followed by QCM-D over a coating time of 24 h.

3.2 Deposition kinetics of tannic acid at pH 6.8 (TA6.8)

Immediately after the coating solution interacted with the crystal surface, a negative frequency shift of -15 Hz was observed. Most likely, this represents the first layer of phenolic molecules coming in contact with and adhering to the titanium oxide surface. The first 5 hours of coating time was characterized by a quick reduction in frequency to $\Delta f \sim 1200$ Hz followed by a slow fall until the frequency leveled off at around -1500 Hz after 15 h deposition time (Figure 5A). This horizontal tendency represents the maximum thickness of the coating. The frequency is stable, and we can therefore assess that no more of the TA molecules adhere to surface at these coating conditions. According to the Sauerbrey model, the deposited coating thickness is 262 nm at 15 hours.

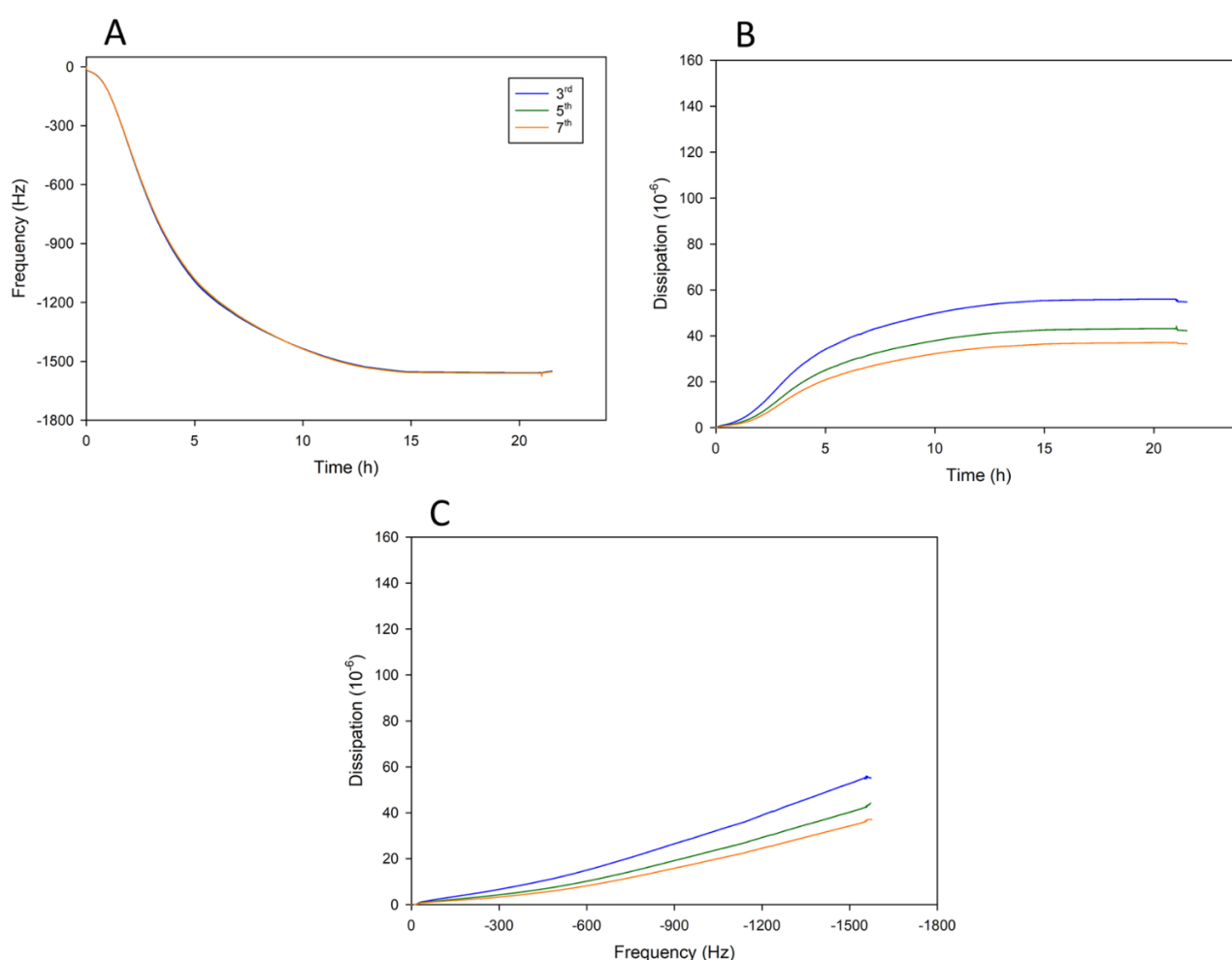


Figure 5: A) Δf -t, B) ΔD -t, and C) $\Delta D - \Delta f$ of TA (pH 6.8) coatings deposited using different flow rates for pumping the coating solution over the quartz crystal.

In the graphs presented in Figure 5, we have three different plots representing the response of the QCM-D sensor to the deposition of TA on its surface. The different resonance harmonics, or overtones, of the signal respond differently to the deposited coating on the sensor surface with

maximum oscillation amplitude decreasing with increasing overtone number (Ohlsson, 2020). This means that the lower overtones are measured further away from the sensor surface while the higher overtones are measured immediately above the titanium surface of the sensor. The coating thickness was modelled using the 3rd overtone of the recorded QCM-D signal, as this overtone represents the signal measured closest to the solid-liquid interface at the coating surface furthest away from the underlying titanium sensor. However, as all overtones presented in the Δf -t plot in Figure 5A are identical, the modelled thickness showed similar values for all measured overtones at each given time.

3.3 Deposition kinetics of tannic acid at pH 7.8 (TA7.8)

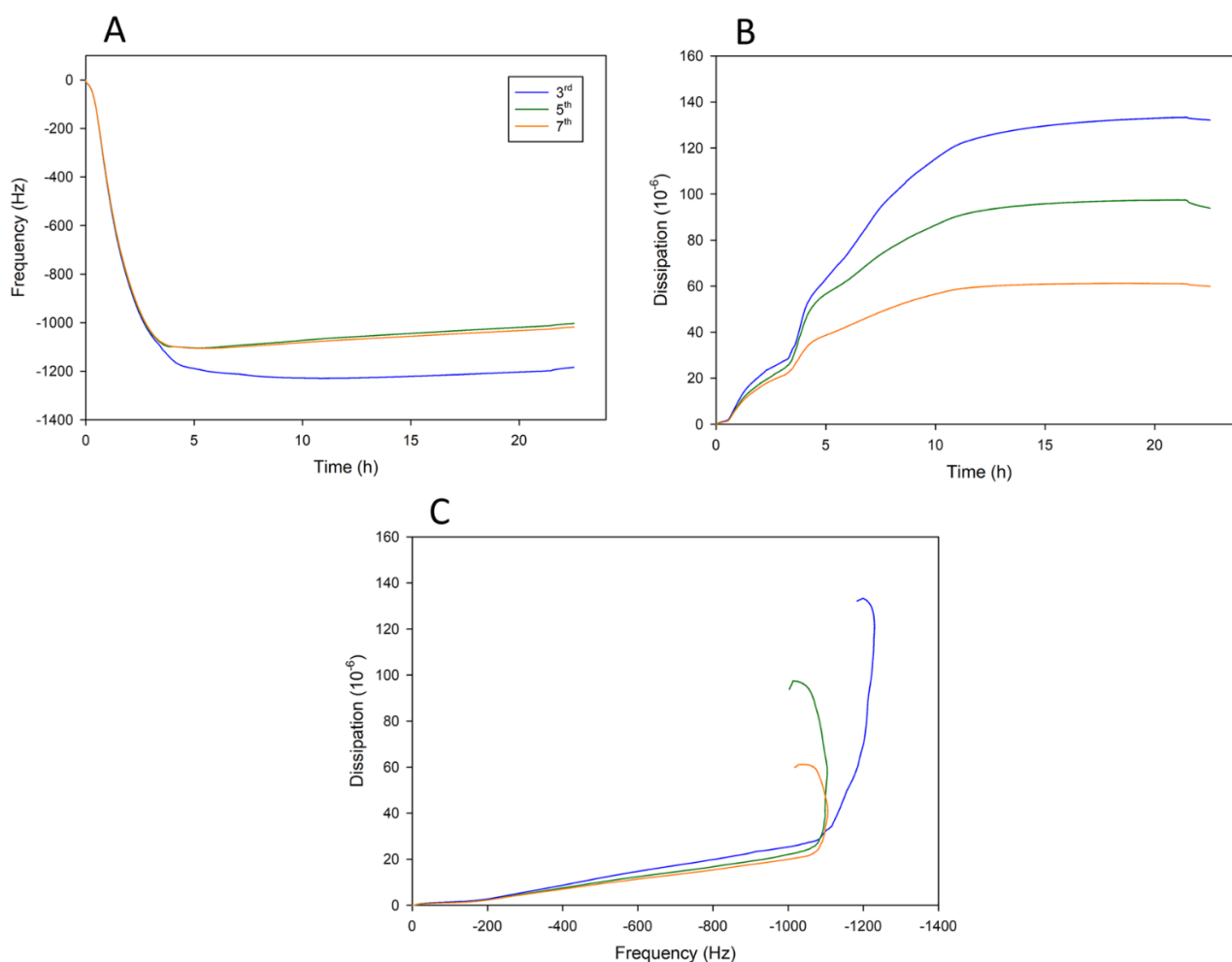


Figure 6: A) Δf -t, B) ΔD -t, and C) $\Delta D - \Delta f$ of TA (pH 7.8) coatings deposited using different flow rates for pumping the coating solution over the quartz crystal

Similar to the TA coatings deposited at pH 6.8, the frequency starts off with a negative frequency shift and a sharp decline of the curve (Figure 6A). The horizontal tendency of the curve happens much

earlier at -1100 Hz after approximately 5 hours of coating time. The maximum thickness of the coating was determined to be 201 nm at the 5 hour mark, according to the Sauerbrey modelling. This marks the end of the mass absorption of the coating.

The dissipation values showed increasingly higher values for the lower overtones (Figure 6B). Here we can assess that this is because the outer layer of the coating is less rigid compared to TA coatings deposited at pH 6.8 as it reacts with more water surrounding the coating closest to the surface. The outer layer will therefore be less densely packed and show different dissipation values (Easley et al., 2022).

Comparing the TA6.8 to the TA7.8, we get a stable coating much faster for the TA7.8 than the TA6.8, after 5 hours and after 15 hours, respectively. Formation a thicker coating was also observed for TA6.8 than for TA7.8 after 15 hours.

Unlike for TA6.8, oxidation reaction is involved in the coating formation of TA7.8 (Sileika et al., 2013). This was also observed during the coating deposition. With increased coating time, the color of the solution used for coating TA7.8 changed from colorless to dark green after approximately 2-3 h (Figure 7). This color change was not occurring for TA6.8 until towards the end of the experiment and the color was not as intense. This difference in oxidation may explain the faster deposition kinetics for TA7.8, resulting in thicker coatings in the initial coating stages. However, the oxidation reaction resulted in faster consumption of the reactive molecules, which led to an earlier end of the mass absorption, and therefore, lower maximum coating thickness.

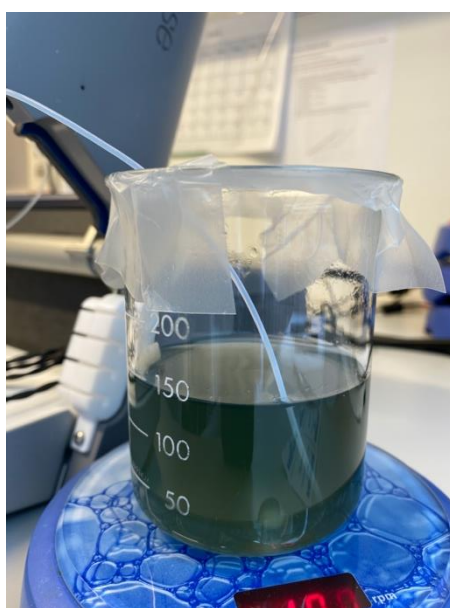


Figure 7: With increasing coating time, the color of the solution altered from colorless to dark green.

3.4 Deposition kinetics of pyrogallol at pH 7.0

The PG coating formation begins with a negative frequency shift of 1-2 Hz, which cannot be seen in Figure 8A due to the scaling of the frequency axis. This is followed by a flat constant slope towards a maximum thickness of approximately 80 nm at frequency -476 Hz after 20 hours (Figure 8A). This resembles the formation of a quite rigid and elastic layer of coating as almost no splitting of the overtones is observed. Furthermore, the frequency values do not level off unlike for TA6.8 and TA7.8 over the 24 h coating time, indicating continuous coating deposition.

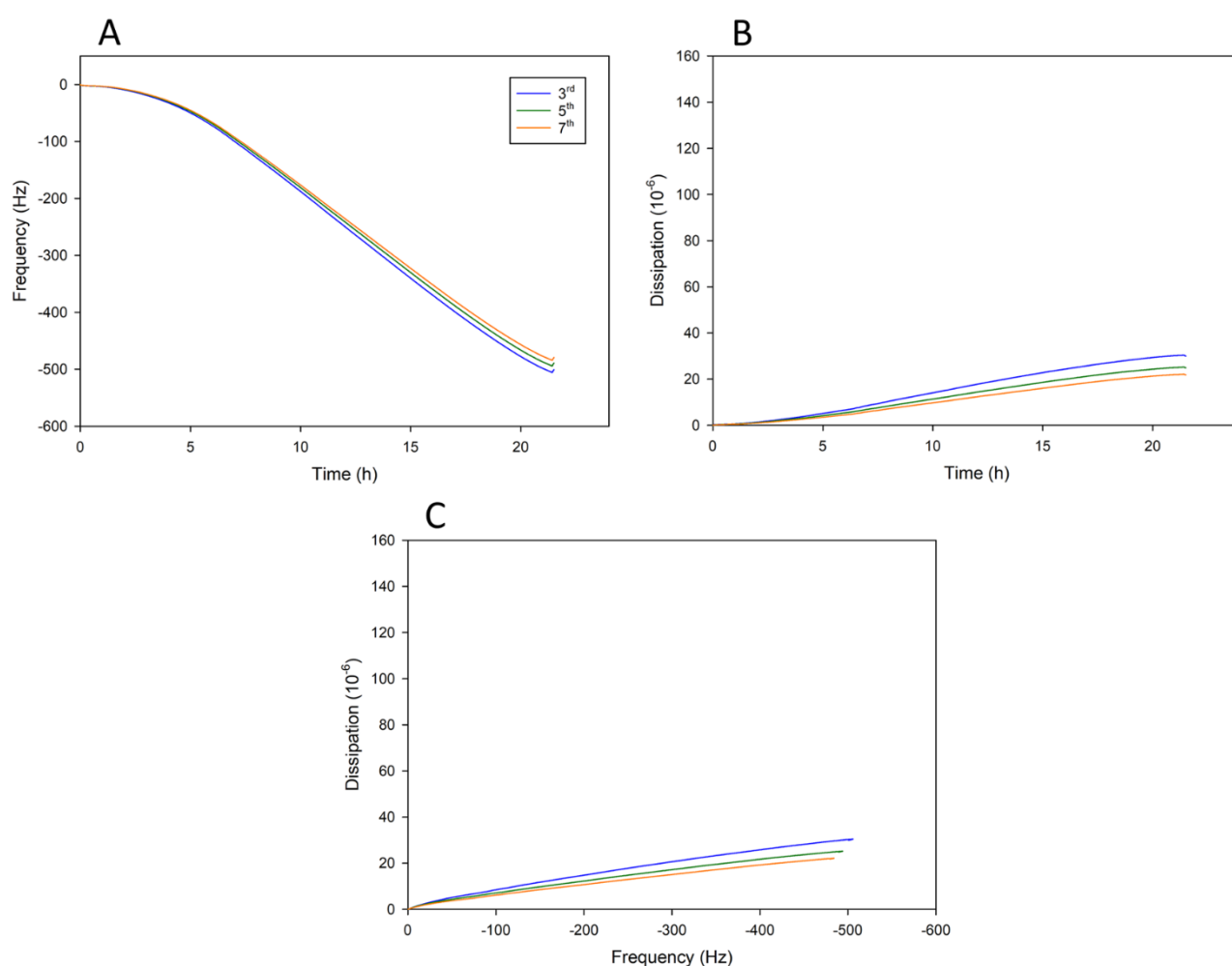


Figure 8: A) Δf -t, B) ΔD -t, and C) $\Delta D - \Delta f$ of PG (pH 7.0) coatings deposited using different flow rates for pumping the coating solution over the quartz crystal

This constant fall of frequency might be attributed to a variety of factors, such as PG (126.11 g/mol) being a significantly smaller molecule as compared to TA (1701.20 g/mol). At 1 mg/ml concentration, TA has approximately 10 times higher molar concentration than PG and there will be 10 times more molecules to react with each other in the PG coating solution compared to the TA. Therefore, the coatings of PG show a steady increase in thickness while also being more rigid in both the outer and

inner regions of the formed coating layer. This is confirmed as the dissipation only increases slightly with increasing thickness and time. (Figure 8B and 8C). The difference in molecular weight also explains the much smaller thickness of the coating. We put the endline of the experiment at 20 hours as after this the time spent would leave the coating formation not cost beneficial for clinical use.

During the coating process, a color change of the PG coating solutions to orange and darkish brown was observed (Figure 9). This confirms the assumed involvement of quinone intermediates in the polymerization response of the phenolic compounds. Polyphenols with one or more ortho-di- or trihydroxyphenyl groups, can go through auto-oxidation at pH values around 7 or above (Haslam, 1998). Oxidative formation of ortho-quinones results in an orange/red color, (Haslam, 1998), which was observed during the study.



Figure 9: The color of the PG solution changed from orange to darkish color.

Furthermore, the processes of complexation for TA and PG may differ. Firstly, simpler phenolic compounds are oxidized to quinones which attribute to a coupled redox system to oxidize more complex polyphenols while they go through a reduction back to the free phenolic state (Haslam, 1998). As a result, when more complex polyphenolic compounds are synthesized during PG auto-oxidation, the quinones produced by PG can be reduced back and remain accessible for future reactions. Such simple phenolic components, on the other hand, are absent from TA solution. There

may be no more or not enough reactive components available to complete the reaction if greater TA complexes were formed.

3.5 Cytotoxicity

The integration of soft tissue performs a critical function for dental implants, since fibroblasts are essential for modifying granular tissue and offer a tight seal of the gingiva to shield the implant from the oral environment (Bainbridge, 2013). Therefore, we investigated whether PG and TA coatings impact hGF response in inflammatory circumstances.

First, the cytotoxicity of both the TA and PG coatings and the precursor molecules dissolved in cell culture medium was assessed using an LDH assay. LDH assay is a method to measure damaged cellular structures (Decker & Lohmann-Matthes, 1988). When the plasma membrane of the cell is damaged, LDH will be released into the cell supernatant (Chan, Moriwaki, & Rosa, 2013). By measuring the activity of LDH in the cell supernatant, the viability of cells can be measured by determining the fraction of viable and dead cells expressed as cytotoxicity (%).

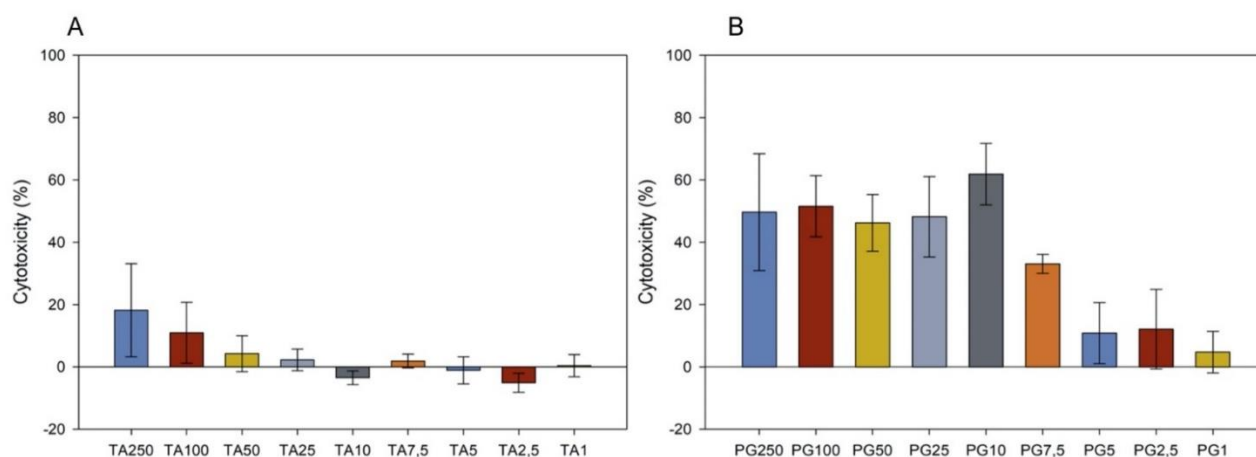


Figure 10: Cytotoxicity of TA and PG on hGFs cell. Cytotoxicity of uncoated (A) dissolved tannic acid and (B) pyrogallol with hGFs as quantified by LDH assay

The cytotoxicity of both dissolved TA and PG on hGFs was increased after 24 hours of cell culture compared to the low control unmodified titanium control surface (Figure 10), showing a response from hGFs to increasing concentration of the polyphenols. For TA concentrations up to 250 µg/ml, the LDH analysis revealed minimal cytotoxicity, only up to an acceptable 20%. PG concentrations over 5 µg/ml exhibited a significant increase in cytotoxicity. This sudden increase in LDH activity observed for cells exposed to PG concentration above 5 µg/ml clearly indicates the cytotoxic threshold for PG in hGF cultures (Figure 10). For TA, no such cytotoxic threshold was detected within

the tested TA concentration range using the LDH assay. Similarly, no cytotoxicity was observed for human gingival fibroblasts cultured on TA and PG coatings (Figure 11), which was associated with the low non-toxic quantities of TA and PG dissolved from the coatings.

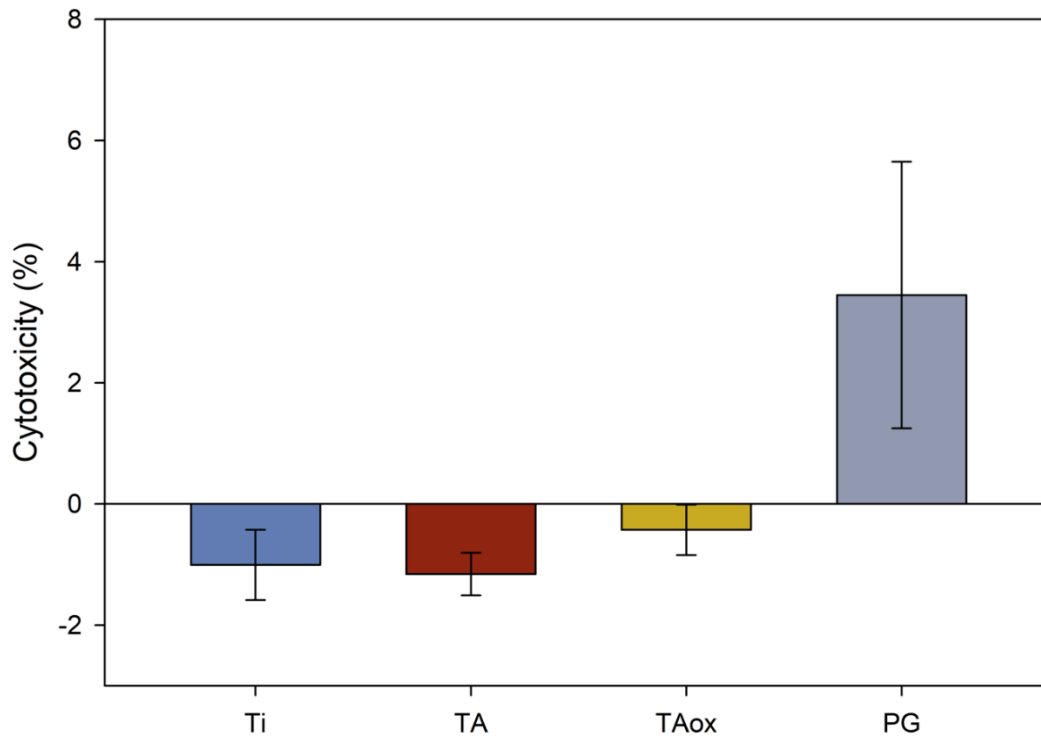


Figure 11: Cytotoxicity of polyphenolic-coated surfaces on hGFs as quantified by LDH assay

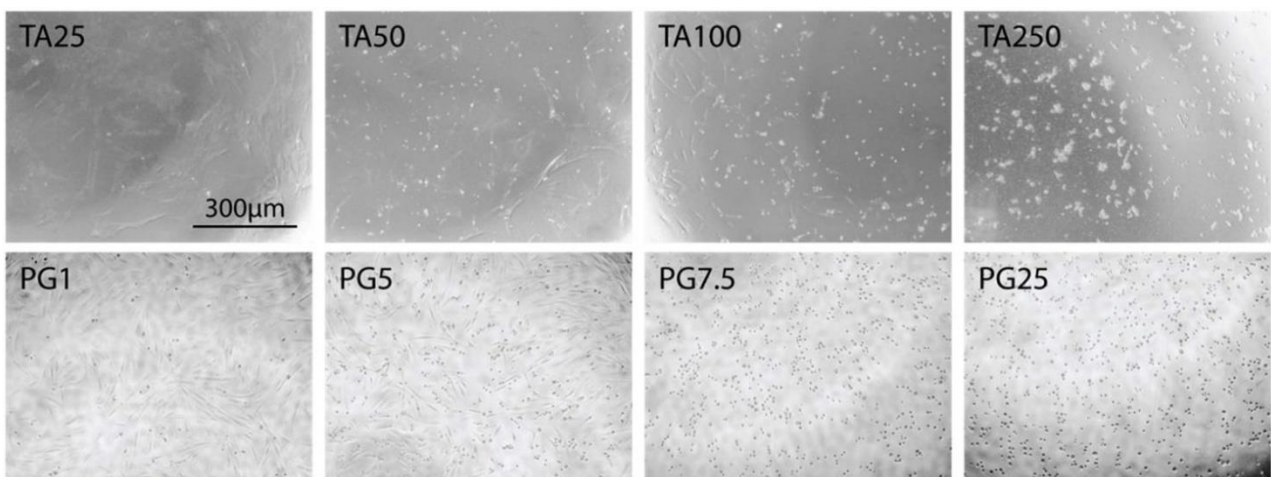


Figure 12: Morphological changes of hGFs after incubation with TA and PG. hGF cultured in DMEM on tissue culture plastic with given amounts of dissolved polyphenols. After 24 hours of incubation at TA concentrations less than 25 $\mu\text{g}/\text{ml}$, excellent cell adherence and phenotypic spreading were observed. The cells took on an increasingly more spherical shape as the TA concentration was increased, and they did not attach effectively to TCP. Likewise, dissolved PG exhibited phenotypical cell form at concentrations less than 5 $\mu\text{g}/\text{ml}$, but an increasingly spherical shape above this value.

In addition to cytotoxicity, cell morphology was assessed by viewing the samples in a phase contrast microscope. This revealed that cells dispersed and adapted the characteristic spindle-shaped cell morphology of viable fibroblasts on surfaces with \leq TA 25 $\mu\text{g/ml}$ and PG \leq 5 g/ml (Figure 12). This was consistent with the LDH results. The 10 times higher molar concentration of PG compared to TA reflects the greater apparent cytotoxic effect. So, it seems to be more cytotoxic than TA since 10-25 $\mu\text{g/ml}$ were still cytotoxic for PG, but not for TA.

These findings suggest that TA and PG coatings as well as dissolved molecules in a low concentration had no detrimental effect on the integrity of the gingival fibroblasts cell membrane. Polyphenolic substances, on the other hand, have the potential to cause irreversible mutations to the DNA (Michałowicz & Duda, 2007). In addition, the substances may also have a pro-oxidant feature, resulting in the formation of reactive oxygen species (ROS) that can induce damage of the DNA and apoptosis (Khan, Ahmad, & Hadi, 2000). Taken together with the reduced cell spreading and adhesion, this implies that the LDH assay is not completely accurate in assessing the cell viability in the presence of polyphenolic molecules.

By performing the LDH assay with dissolved polyphenols in the cell culture medium, we were able to determine the cytotoxic concentration of the polyphenols to the human gingival fibroblasts. This was important since we wanted to observe if the coatings can have an anti-inflammatory effect. We wanted to assess whether the coatings will inherit the anti-inflammatory properties of the molecules they are built up from. Coating formation can alter the chemical structure of the precursor molecules, and thereby, alter their biological activity. Although tannic acid and pyrogallol in solution have been shown to elicit antioxidant and anti-inflammatory properties (Jang et al., 2013), (Rahman et al., 2006), (Zhan et al., 2016), coatings composed of these molecules do not necessarily have the same effect. To determine the biological effect of the TA and PG nanocoatings, their impact on cultured cells should therefore be compared to that of the precursor molecules themselves. Thus, the purpose of the cytotoxicity assessment was to confirm that the coatings are not toxic against the human gingival fibroblasts, as well as determine the greatest concentration of TA/PG that the cells may be exposed to without being cytotoxic.

3.6 Inflammatory markers

Decreased IL-6 gene expression has recently been observed for human gingival fibroblasts cultured on titanium surfaces with covalently bound polyphenols, an effect that has been attributed to the anti-inflammatory properties of such polyphenol modified surfaces (Córdoba et al., 2015). We therefore

measured four inflammatory markers that are the most relevant for inflammation. These were secreted in a culture medium from hGFs and induced with inflammation by LPS and IL- β . C- was therefore cells grown on TCP without LPS + IL-1 β and C+ is cells grown with LPS + IL-1 β .

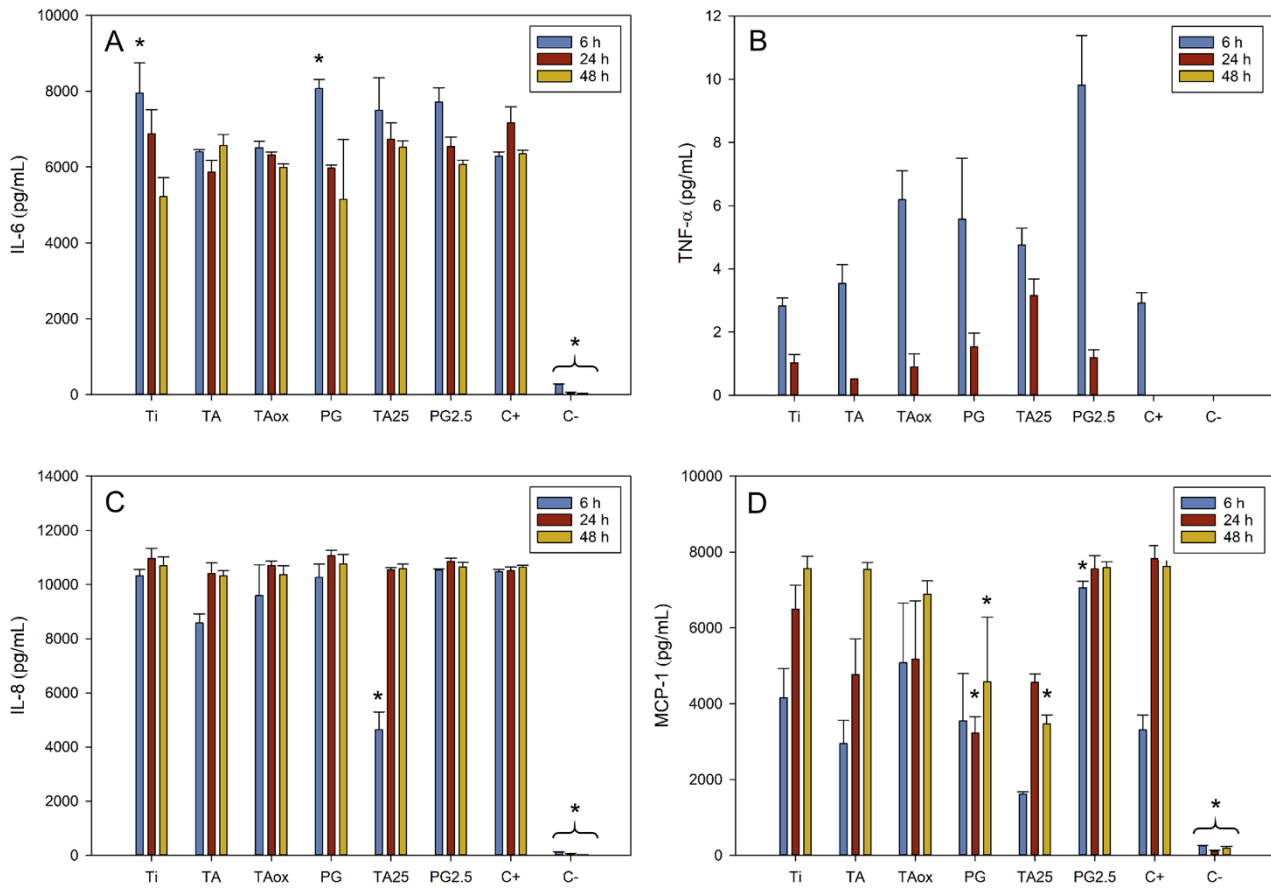


Figure 13: Using a multiplex (Luminex) assay cells that were inflamed with LPS and IL-1 was analyzed after 6, 24 and 48 h for the expression of IL-6, TNF- α , IL-8 and MCP-1. Values are presented as mean \pm SD. * p < 0.05 compared to C+ at the corresponding timepoint.

On Ti surface, hGFs showed high levels of IL-6, IL-8 and MCP-1 all around (Figure 13). This is in good agreement with reported response of hGFs to IL-1 β and LPS derived from *P. gingivalis* (Agarwal et al., 1995). The detected TNF- α levels were below the detection limit between 24 - 48 h and are therefore not plotted in Figure 13B. Neither dissolved polyphenols nor the modified surfaces affected the inflammatory response 24 h after stimulation with LPS/IL-1 β (Figure 13). Similar observation was made 6 h and 48 h after inducing inflammation.

Overall, the polyphenolic coatings did not induce a significant change in expression of any cytokines, and PG-coated samples actually upregulated the presence of IL-6 and MCP-1 above the C+ after 24 h. Contrary to our results, other studies have found that plant polyphenols containing pyrogallol and catechol groups reduced the expression of pro-inflammatory cytokines in various human cells stimulated by LPS (Pan, Lin-Shiau, Ho, Lin, & Lin, 2000), (Xiong et al., 2019), (Wheeler et al., 2004), (Grenier, Chen, Ben Lagha, Fournier-Larente, & Morin, 2015). In these studies, however they only stimulated the cells with LPS, whereas we stimulated them with both IL-1 β and LPS which might also be a factor in our coatings' inability to curb inflammation. Why this is not presented in the results of this study might have something to do with the hGFs used, a source of error in the experiments or that polyphenols coated on Ti surfaces somehow do not express the same anti-inflammatory effects as seen in earlier experiments with uncoated polyphenols.

3.7 NF- κ B activation

Since the expression of the pro-inflammatory cytokines upon exposure to LPS and IL-1 β has been associated with NF- κ B signaling pathways (Ma, Ge, Zhang, & Lin, 2017), we investigated whether TA and PG affect NF- κ B signal transduction. We found equal level of phosphorylation of NF- κ B p65 in hGFs for all tested samples 24 hours after induction of inflammation with elevated values for TA and PG.

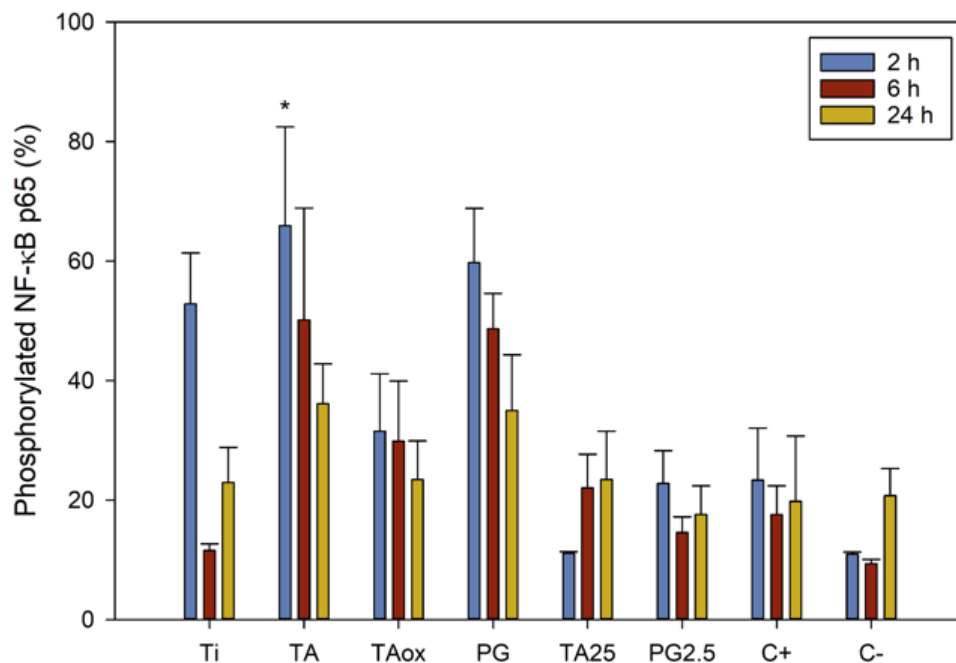


Figure 14: NF- κ B activation in hGFs. Ratio of phosphorylated to total NF- κ B p65 in hGFs 2, 6 and 24 h after inflammation by LPS and IL-1 β . Concentrations for dissolved polyphenols were 250 μ g/ml TA and 5 g/ml PG. Results are presented as mean \pm SD. * $p < 0.05$ compared to C+ at the corresponding timepoint.

Contrary to previous studies, (Pan et al., 2000), (Xiong et al., 2019), (Wheeler et al., 2004), (Grenier et al., 2015), (Jang et al., 2013), dissolved TA and PG did not reduce NF- κ B phosphorylation, which clearly correlated with the cytokine / inflammatory markers expression (Figure 14). Based on our results, neither the coatings nor the dissolved TA or PG could inhibit the inflammatory response either due to the hGFs and combination of inflammatory stimuli we used, or due to a low concentration of released or dissolved polyphenols.

3.8 Cell morphology

Before fluorescence imaging, the cells adhering to the coins were stained with DAPI and Alexa phalloidin to analyze the quantity and shape of the cells. The nuclei of the cells were stained with DAPI, while the actin filaments of the cells are stained with phalloidin (Li, Bai, Sakai, & Hashikawa, 2009).

After 48 hours, human gingival fibroblasts sown on treated titanium coins (Ti) demonstrated excellent adherence and spreading, as shown in Figure 15. We clearly see a difference between the control and inflamed Ti surface, where the cells are less frequent with a round circular shape and less cytoskeleton. By comparing the control and inflamed conditions, we did not observe change in the cell morphology for TA and TA_{ox}. However, no actin filaments were detected in the inflamed cells on the PG surfaces. These findings may indicate that the TA has better anti-inflammatory effects than the PG coatings, despite the lack of reduction in pro-inflammatory markers detected for any of the polyphenolic surfaces in this study.

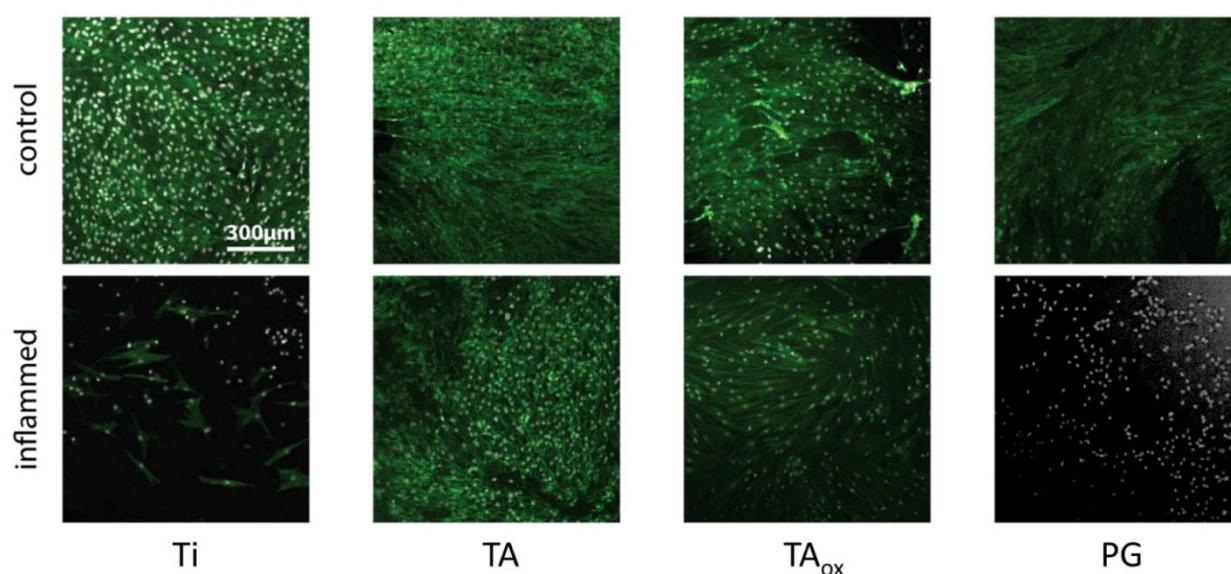


Figure 15: Cell morphology of human gingival fibroblast cultured in the absence (control) or presence (inflammation) pro-inflammatory stimuli LPS and IL-1 β . Gray: nuclei, green: cytoskeletons.

4 Conclusions

In this study we investigated the effects of TA and PG coating formation and the ability to reduce inflammatory cytokines when sampled together with human gingival fibroblasts.

We decided the concentration of polyphenols by analyzing cytotoxicity of the hGFs and found that 25 $\mu\text{g/ml}$ of TA and 2.5 g/ml of PG showed the least amount of cell death while having the highest concentration of dissolved polyphenolic molecules hGFs can be exposed before adverse effects on cell behavior were observed. This was confirmed by LHD assay in combination with viewing the cells in a microscope examining the cell morphology from phenotypical shapes to spherical above these concentrations.

The phase contrast images showed that the cells started to look more rounded at lower concentrations than where we saw the increase in LDH activity. This could probably be due to that the LDH is depending on damaging of the plasma membrane. However, nanocoatings of PG and TA were found to be cytocompatible and human gingival fibroblasts were adhered and spread evenly on coated Ti surface.

Upon inflammation of hGFs with LPS/IL-1 β the polyphenolic coatings were not able to reduce the expression of pro-inflammatory cytokines. This was linked to the activation of the NF- κ B p65 signaling pathway. Since inflammatory responses and signaling pathways are complex cell-specific processes, further studies are needed to evaluate the ability of polyphenolic surface modifications to support early wound closing and fibroblast adhesion.

5 References

- Abrahamsson, I., Berglundh, T., Linder, E., Lang, N. P., & Lindhe, J. (2004). Early bone formation adjacent to rough and turned endosseous implant surfaces: an experimental study in the dog. *Clinical oral implants research*, 15(4), 381-392.
- Adell, R., Lekholm, U., Rockler, B., & Brånemark, P.-I. (1981). A 15-year study of osseointegrated implants in the treatment of the edentulous jaw. *International journal of oral surgery*, 10(6), 387-416.
- Agarwal, S., Baran, C., Piesco, N., Quintero, J., Langkamp, H., Johns, L., & Chandra, C. (1995). Synthesis of proinflammatory cytokines by human gingival fibroblasts in response to lipopolysaccharides and interleukin-1 β . *Journal of periodontal research*, 30(6), 382-389.
- Allen, P. F. (2003). Assessment of oral health related quality of life. *Health and quality of life outcomes*, 1(1), 1-8.
- Antoniak, S. (2018). The coagulation system in host defense. *Research and Practice in Thrombosis and Haemostasis*, 2(3), 549-557.
- Anusavice, K. J., Shen, C., & Rawls, H. R. (2012). *Phillips' science of dental materials*: Elsevier Health Sciences.
- Aubrey, S., & Gopalakrishnan, S. N. (2002). Periodontal diseases in Europe. *Periodontology 2000*, 29, 104-121.
- Bainbridge, P. (2013). Wound healing and the role of fibroblasts. *Journal of wound care*, 22(8).
- Barrett, D. G., Sileika, T. S., & Messersmith, P. B. (2014). Molecular diversity in phenolic and polyphenolic precursors of tannin-inspired nanocoatings. *Chemical communications*, 50(55), 7265-7268.
- Barrientos, S., Stojadinovic, O., Golinko, M. S., Brem, H., & Tomic-Canic, M. (2008). Growth factors and cytokines in wound healing. *Wound repair and regeneration*, 16(5), 585-601.

- Bodet, C., Chandad, F., & Grenier, D. (2007). Cranberry components inhibit interleukin-6, interleukin-8, and prostaglandin E2 production by lipopolysaccharide-activated gingival fibroblasts. *European journal of oral sciences*, 115(1), 64-70.
- Bosshardt, D. D., Chappuis, V., & Buser, D. (2017). Osseointegration of titanium, titanium alloy and zirconia dental implants: current knowledge and open questions. *Periodontology 2000*, 73(1), 22-40.
- Boyan, B. D., Hummert, T. W., Dean, D. D., & Schwartz, Z. (1996). Role of material surfaces in regulating bone and cartilage cell response. *Biomaterials*, 17(2), 137-146.
- Byrne, G. (2014). *Fundamentals of implant dentistry*: John Wiley & Sons.
- Campoccia, D., Montanaro, L., & Arciola, C. R. (2013). A review of the biomaterials technologies for infection-resistant surfaces. *Biomaterials*, 34(34), 8533-8554.
- Camps-Font, O., González-Barnadas, A., Mir-Mari, J., Figueiredo, R., Gay-Escoda, C., & Valmaseda-Castellón, E. (2020). Fracture resistance after implantoplasty in three implant-abutment connection designs. *Medicina Oral, Patología Oral y Cirugía Bucal*, 25(5), e691.
- Carcuac, O., Derks, J., Charalampakis, G., Abrahamsson, I., Wennström, J., & Berglundh, T. (2016). Adjunctive systemic and local antimicrobial therapy in the surgical treatment of peri-implantitis: a randomized controlled clinical trial. *Journal of dental research*, 95(1), 50-57.
- Chan, F. K.-M., Moriwaki, K., & Rosa, M. J. D. (2013). Detection of necrosis by release of lactate dehydrogenase activity. In *Immune Homeostasis* (pp. 65-70): Springer.
- Chen, L., Deng, H., Cui, H., Fang, J., Zuo, Z., Deng, J., . . . & Zhao, L. (2018). Inflammatory responses and inflammation-associated diseases in organs. In: *Oncotarget*.
- Chen, X., Li, Y., & Aparicio, C. (2013). Biofunctional coatings for dental implants. In *Thin films and coatings in biology* (pp. 105-143): Springer.
- Córdoba, A., Satué, M., Gómez-Florit, M., Hierro-Oliva, M., Petzold, C., Lyngstadaas, S. P., . . . Ramis, J. M. (2015). Flavonoid-modified surfaces: multifunctional bioactive biomaterials

with osteopromotive, anti-inflammatory, and anti-fibrotic potential. *Advanced Healthcare Materials*, 4(4), 540-549.

Cosyn, J., Sabzevar, M. M., De Wilde, P., & De Rouck, T. (2007). Commentary: Two-Piece Implants With Turned Versus Microtextured Collars. *Journal of Periodontology*, 78(9), 1657-1663.

Decker, T., & Lohmann-Matthes, M.-L. (1988). A quick and simple method for the quantitation of lactate dehydrogenase release in measurements of cellular cytotoxicity and tumor necrosis factor (TNF) activity. *Journal of immunological methods*, 115(1), 61-69.

Donachie, M. J. (2000). *Titanium: a technical guide*: ASM international.

Easley, A. D., Ma, T., Eneh, C. I., Yun, J., Thakur, R. M., & Lutkenhaus, J. L. (2022). A practical guide to quartz crystal microbalance with dissipation monitoring of thin polymer films. *Journal of Polymer Science*, 60(7), 1090-1107.

Elias, C. N., & Meirelles, L. (2010). Improving osseointegration of dental implants. *Expert review of medical devices*, 7(2), 241-256.

Esposito, M., Hirsch, J.-M., Lekholm, U., & Thomsen, P. (1997). Failure patterns of four osseointegrated oral implant systems. *Journal of Materials Science: Materials in Medicine*, 8(12), 843-847.

Feghali, K., Feldman, M., La, V. D., Santos, J., & Grenier, D. (2012). Cranberry proanthocyanidins: natural weapons against periodontal diseases. *Journal of agricultural and food chemistry*, 60(23), 5728-5735.

Geißler, S., Barrantes, A., Tengvall, P., Messersmith, P. B., & Tiainen, H. (2016). Deposition kinetics of bioinspired phenolic coatings on titanium surfaces. *Langmuir*, 32(32), 8050-8060.

Gerritsen, A. E., Allen, P. F., Witter, D. J., Bronkhorst, E. M., & Creugers, N. H. (2010). Tooth loss and oral health-related quality of life: a systematic review and meta-analysis. *Health and quality of life outcomes*, 8(1), 1-11.

- Grenier, D., Chen, H., Ben Lagha, A., Fournier-Larente, J., & Morin, M.-P. (2015). Dual action of myricetin on *Porphyromonas gingivalis* and the inflammatory response of host cells: a promising therapeutic molecule for periodontal diseases. *PLOS ONE*, *10*(6), e0131758. doi:10.1371/journal.pone.0131758
- Gruber, R., & Bosshardt, D. D. (2015). Dental Implantology and Implants-Tissue Interface. In *Stem Cell Biology and Tissue Engineering in Dental Sciences* (pp. 735-747): Elsevier.
- Haslam, E. (1998). *Practical polyphenolics: from structure to molecular recognition and physiological action*: Cambridge University Press.
- Heemskerk, J. W., Bevers, E. M., & Lindhout, T. (2002). Platelet activation and blood coagulation. *Thrombosis and haemostasis*, *88*(08), 186-193.
- Höök, F., Vörös, J., Rodahl, M., Kurrat, R., Böni, P., Ramsden, J., . . . Gold, J. (2002). A comparative study of protein adsorption on titanium oxide surfaces using in situ ellipsometry, optical waveguide lightmode spectroscopy, and quartz crystal microbalance/dissipation. *Colloids and Surfaces B: Biointerfaces*, *24*(2), 155-170.
- Jang, S. E., Hyam, S. R., Jeong, J. J., Han, M. J., & Kim, D. H. (2013). Penta-O-galloyl- β -D-glucose ameliorates inflammation by inhibiting MyD 88/NF- κ B and MyD 88/MAPK signalling pathways. *British journal of pharmacology*, *170*(5), 1078-1091.
- Javed, F., AlGhamdi, A. S. T., Ahmed, A., Mikami, T., Ahmed, H. B., & Tenenbaum, H. C. (2013). Clinical efficacy of antibiotics in the treatment of peri-implantitis. *International dental journal*, *63*(4), 169-176.
- Johannsmann, D. (2015). The quartz crystal microbalance in soft matter research. *Soft and Biological Matter*, 191-204.
- Johnson, R. W. (1997). Inhibition of growth by pro-inflammatory cytokines: an integrated view. *Journal of animal science*, *75*(5), 1244-1255.
- Khan, N. S., Ahmad, A., & Hadi, S. (2000). Anti-oxidant, pro-oxidant properties of tannic acid and its binding to DNA. *Chemico-Biological Interactions*, *125*(3), 177-189.

- Krebs, M., Kesar, N., Begić, A., von Krockow, N., Nentwig, G. H., & Weigl, P. (2019). Incidence and prevalence of peri-implantitis and peri-implant mucositis 17 to 23 (18.9) years postimplant placement. *Clinical implant dentistry and related research*, 21(6), 1116-1123.
- Lang, N. P. (2019). Oral implants: the paradigm shift in restorative dentistry. *Journal of dental research*, 98(12), 1287-1293.
- Li, Y.-C., Bai, W.-Z., Sakai, K., & Hashikawa, T. (2009). Fluorescence and electron microscopic localization of F-actin in the ependymocytes. *Journal of Histochemistry & Cytochemistry*, 57(8), 741-751.
- Lie, S., Lygre, G., Reichhelm, I., Eggum, E., Bull, V., & Gjengedal, H. (2019). Data fra Helfo og Norsk pasientskadeerstatning gir liten informasjon om kvalitet og omfang av behandling med tannimplantater i Norge. *Nor Tannlegeforen Tid*, 129, 776-782.
- Ma, T., Ge, X., Zhang, Y., & Lin, Y. (2017). Effect of titanium surface modifications of dental implants on rapid osseointegration. In *Interface Oral Health Science 2016* (pp. 247-256): Springer, Singapore.
- Merle, N. S., Church, S. E., Fremeaux-Bacchi, V., & Roumenina, L. T. (2015). Complement System Part I—Molecular Mechanisms of Activation and Regulation, *Front Immunol* 6 (2015) 262. In.
- Merle, N. S., Noe, R., Halbwachs-Mecarelli, L., Fremeaux-Bacchi, V., & Roumenina, L. T. (2015). Complement system part II: role in immunity. *Frontiers in immunology*, 6, 257.
- Michałowicz, J., & Duda, W. (2007). Phenols--Sources and Toxicity. *Polish Journal of Environmental Studies*, 16(3).
- Mombelli, A. (2002). Microbiology and antimicrobial therapy of peri-implantitis. *Periodontology* 2000, 28(1), 177-189.
- Mombelli, A., Müller, N., & Cionca, N. (2012). The epidemiology of peri-implantitis. *Clinical oral implants research*, 23, 67-76.

- Moraschini, V., Poubel, L. d. C., Ferreira, V., & dos Sp Barboza, E. (2015). Evaluation of survival and success rates of dental implants reported in longitudinal studies with a follow-up period of at least 10 years: a systematic review. *International journal of oral and maxillofacial surgery*, *44*(3), 377-388.
- Neumann, M., & Naumann, M. (2007). Beyond I κ Bs: alternative regulation of NF- κ B activity. *The FASEB Journal*, *21*(11), 2642-2654.
- Ohlsson, G. (2020). Why it is useful to use multiple overtones in QCM measurements.
- Osman, R. B., & Swain, M. V. (2015). A critical review of dental implant materials with an emphasis on titanium versus zirconia. *Materials*, *8*(3), 932-958.
- Palaska, I., Papathanasiou, E., & Theoharides, T. C. (2013). Use of polyphenols in periodontal inflammation. *European journal of pharmacology*, *720*(1-3), 77-83.
- Pan, M.-H., Lin-Shiau, S.-Y., Ho, C.-T., Lin, J.-H., & Lin, J.-K. (2000). Suppression of lipopolysaccharide-induced nuclear factor- κ B activity by theaflavin-3, 3'-digallate from black tea and other polyphenols through down-regulation of I κ B kinase activity in macrophages. *Biochemical pharmacology*, *59*(4), 357-367.
- Perez-Chaparro, P., Gonçalves, C., Figueiredo, L., Faveri, M., Lobão, E., Tamashiro, N., . . . Feres, M. (2014). Newly identified pathogens associated with periodontitis: a systematic review. *Journal of dental research*, *93*(9), 846-858.
- Polizzi, G., Grunder, U., Goené, R., Hatano, N., Henry, P., Jackson, W. J., . . . Triplett, G. (2000). Immediate and delayed implant placement into extraction sockets: a 5-year report. *Clinical implant dentistry and related research*, *2*(2), 93-99.
- Pålsson-McDermott, E. M., & O'Neill, L. A. (2004). Signal transduction by the lipopolysaccharide receptor, Toll-like receptor-4. *Immunology*, *113*(2), 153-162.
- Quideau, S., Deffieux, D., Douat-Casassus, C., & Pouységu, L. (2011). Plant polyphenols: chemical properties, biological activities, and synthesis. *Angewandte Chemie International Edition*, *50*(3), 586-621.

- Rahman, I., Biswas, S. K., & Kirkham, P. A. (2006). Regulation of inflammation and redox signaling by dietary polyphenols. *Biochemical pharmacology*, 72(11), 1439-1452.
- Sanjabi, S., Zenewicz, L. A., Kamanaka, M., & Flavell, R. A. (2009). Anti-inflammatory and pro-inflammatory roles of TGF- β , IL-10, and IL-22 in immunity and autoimmunity. *Current opinion in pharmacology*, 9(4), 447-453.
- Schwarz, F., Derks, J., Monje, A., & Wang, H. L. (2018). Peri-implantitis. *Journal of clinical periodontology*, 45, S246-S266.
- Serhan, C. N., Ward, P. A., & Gilroy, D. W. (2010). *Fundamentals of inflammation*: Cambridge University Press.
- Sileika, T. S., Barrett, D. G., Zhang, R., Lau, K. H. A., & Messersmith, P. B. (2013). Colorless multifunctional coatings inspired by polyphenols found in tea, chocolate, and wine. *Angewandte Chemie*, 125(41), 10966-10970.
- Turri, A., Orlando Rossetti, P. H., Canullo, L., Grusovin, M. G., & Dahlin, C. (2016). Prevalence of Peri-implantitis in Medically Compromised Patients and Smokers: A Systematic Review. *International Journal of Oral & Maxillofacial Implants*, 31(1).
- Van Noort, R. (1987). Titanium: the implant material of today. *Journal of Materials Science*, 22(11), 3801-3811.
- Vos, T., Abajobir, A. A., Abate, K. H., Abbafati, C., Abbas, K. M., Abd-Allah, F., . . . Abera, S. F. (2017). Global, regional, and national incidence, prevalence, and years lived with disability for 328 diseases and injuries for 195 countries, 1990–2016: a systematic analysis for the Global Burden of Disease Study 2016. *The Lancet*, 390(10100), 1211-1259.
- Weber, F. (2021). Development of Multifunctional Polyphenolic Coatings for Improved Peri-Implant Healing.
- Wheeler, D. S., Catravas, J. D., Odoms, K., Denenberg, A., Malhotra, V., & Wong, H. R. (2004). Epigallocatechin-3-gallate, a green tea-derived polyphenol, inhibits IL-1 β -dependent

proinflammatory signal transduction in cultured respiratory epithelial cells. *The Journal of nutrition*, 134(5), 1039-1044.

Williams, D. F. (1976). Corrosion of implant materials. *Annual review of materials science*, 6(1), 237-266.

Xiong, G., Ji, W., Wang, F., Zhang, F., Xue, P., Cheng, M., . . . Zhang, T. (2019). Quercetin inhibits inflammatory response induced by LPS from *Porphyromonas gingivalis* in human gingival fibroblasts via suppressing NF- κ B signaling pathway. *Biomed Research International*, 2019.

Zhan, K., Ejima, H., & Yoshie, N. (2016). Antioxidant and adsorption properties of bioinspired phenolic polymers: A comparative study of catechol and gallol. *ACS Sustainable Chemistry & Engineering*, 4(7), 3857-3863.

Zhao, B., Van Der Mei, H. C., Subbiahdoss, G., de Vries, J., Rustema-Abbing, M., Kuijper, R., . . . Ren, Y. (2014). Soft tissue integration versus early biofilm formation on different dental implant materials. *Dental materials*, 30(7), 716-727.

Zitzmann, N. U., & Berglundh, T. (2008). Definition and prevalence of peri-implant diseases. *Journal of clinical periodontology*, 35, 286-291.

6 Appendix


Characterization of the foreign body response of titanium implants modified with polyphenolic coatings

Weber F, Quach HQ, Reiersen M, Sarraj SY, Bakir DN, Jankowski VA, Nilsson PH, Tiainen H.

Published in: *J Biomed Mater Res A*, 2022, 110, 1341-1355.

RESEARCH ARTICLE

Characterization of the foreign body response of titanium implants modified with polyphenolic coatings

Florian Weber¹ | Huy Quang Quach² | Mathias Reiersen¹ | Sadaf Yosef Sarraj¹ |
 Dyala Nidal Bakir¹ | Victor Aleksander Jankowski¹ | Per H. Nilsson^{2,3} |
 Hanna Tiainen¹ 

¹Department of Biomaterials, Institute of Clinical Dentistry, University of Oslo, Oslo, Norway

²Department of Immunology, Institute of Clinical Medicine, University of Oslo, Oslo, Norway

³Department of Chemistry and Biomedical Sciences, Linnaeus University, Kalmar, Sweden

Correspondence

Hanna Tiainen, Department of Biomaterials, Institute of Clinical Dentistry, University of Oslo, Oslo, Norway.

Email: hanna.tiainen@odont.uio.no

Funding information

Research Council of Norway, Grant/Award Numbers: 274332, 302590

Abstract

The foreign body response is dictating the outcome of wound healing around any implanted materials. Patients who suffer from chronic inflammatory diseases and impaired wound healing often face a higher risk for implant failure. Therefore, functional surfaces need to be developed to improve tissue integration. For this purpose, we evaluated the impact of surface coatings made of antioxidant polyphenolic molecules tannic acid (TA) and pyrogallol (PG) on the host response in human blood. Our results showed that although the polyphenolic surface modifications impact the initial blood protein adsorption compared to Ti, the complement and coagulation systems are triggered. Despite complement activation, monocytes and granulocytes remained inactivated, which was manifested in a low pro-inflammatory cytokine expression. Under oxidative stress, both coatings were able to reduce intracellular reactive oxygen species in human gingival fibroblasts (hGFs). However, no anti-inflammatory effects of polyphenolic coatings could be verified in hGFs stimulated with lipopolysaccharide and IL-1 β . Although polyphenols reportedly inhibit the NF- κ B signaling pathway, phosphorylation of NF- κ B p65 was observed. In conclusion, our results indicated that TA and PG coatings improved the hemocompatibility of titanium surfaces and have the potential to reduce oxidative stress during wound healing.

KEYWORDS

antioxidant, blood, fibroblasts, pyrogallol, surface modification, tannic acid, wound healing

Abbreviations: ABTS, 2,2'-azino-bis(3-ethylbenzothiazoline-6-sulfonic acid); DMEM, Dulbecco's modified Eagles medium; F1 + 2, prothrombin fragment 1 + 2; GA, gallic acid; hGF, human gingival fibroblast; IgG, immunoglobulin G; IL, interleukin; LDH, lactate dehydrogenase; LPS, (bacteria derived) lipopolysaccharide; MCP-1, monocyte chemoattractant protein 1; NF- κ B, nuclear factor kappa B; PBS, phosphate buffered saline; PG, pyrogallol; PG 70, PG coating obtained at pH = 7.0; PGG, penta-galloyl glucose; ROS, reactive oxygen species; QCM-D, quartz crystal microbalance with dissipation monitoring; TA, tannic acid; TA 68, TA coating obtained at pH = 6.8; TA 78, TA coating obtained at pH = 7.8; TAT, thrombin-antithrombin complex; TBHP, tert-butyl hydroperoxide; TCC, terminal complement complex; TCP, tissue culture plastic; TEAC, trolox equivalent activity concentration.

1 | INTRODUCTION

Titanium (Ti) is a widespread material in medical applications due to its mechanical properties and corrosion resistance.¹ Further, a firm tissue integration and low foreign body response has made titanium and its alloys a popular choice as material for bone anchored implants and cardiovascular applications.² Particularly for transcutaneous and transmucosal implants, such as auricular or dental implants, their

This is an open access article under the terms of the [Creative Commons Attribution](https://creativecommons.org/licenses/by/4.0/) License, which permits use, distribution and reproduction in any medium, provided the original work is properly cited.

© 2022 The Authors. *Journal of Biomedical Materials Research Part A* published by Wiley Periodicals LLC.

clinical success strongly relies on their integration in the surrounding hard and soft tissues.³ With the natural skin barrier impaired, infections caused by bacteria often lead to failure of the implant.^{4,5} Commonly, challenges in tissue integration and wound healing processes have addressed the hard tissue, but efforts need to be made to also improve the soft tissue integration.^{6,7}

Wound healing around implants starts with the direct contact with blood. The immediate adsorption of plasma proteins onto the implant surface dictates the subsequent activation of immune cells, the complement system, and the coagulation cascade.⁸ Thus, control of the foreign body reaction towards implants results in faster wound healing and close contact between the peri-implant tissue and the implant surface can therefore be established during the subsequent resolution of the inflammatory phase. Thereby, the entry of potential pathogenic microbes to the wound site and colonization of the implant surface can be prevented.⁹

A variety of different surface modification strategies have emerged to improve the tissue integration of titanium implants. With respect to dental implants, approaches to change the surface topography and its physical, chemical, and biological properties have been studied.⁷ The underlying aim is to modulate protein adsorption, cell responses, and the microbial colonization of the implant surface. Among the chemical and biological surface modifications, changes of surface charge and hydrophilic properties, or functionalization with different bioactive molecules have been explored.¹⁰ Recently, polyphenolic molecules have been suggested as potential candidates to tackle inflammation and reduce microbial colonization.¹¹ Their anti-inflammatory properties are attributed to their capability to reduce oxidative stress,¹² which is based on catechol and gallol units. These structures are able to scavenge radicals and redox active ions.¹³ In addition, polyphenols can reduce inflammation via modulating cellular signaling pathways.¹⁴ In particular, inhibition of I κ B kinase on the nuclear factor κ B (NF- κ B) signaling pathway in macrophages has been reported for several polyphenolic molecules.^{15–17} Similarly, inhibition of pro-inflammatory cytokine expression by polyphenols has been shown in gingival fibroblasts exposed to bacterial lipopolysaccharide (LPS).¹⁸ Therefore, a variety of polyphenolic molecules have been suggested as treatment options for patients with inflammatory periodontal diseases.^{19,20}

Since certain polyphenols are able to form surface coatings,²¹ this property may be harnessed for local delivery of active molecules in the peri-implant environment. For example, Ti surfaces modified with dopamine, quercetin, curcumin, and tannic acid (TA) have shown osteopromotive and anti-inflammatory effects on various cell types *in vitro*.^{22–26}

Despite their potential to modulate the foreign body response, polyphenolic surface modifications have so far not been systematically investigated for early wound healing processes in soft tissues. Therefore, we evaluated the effect of TA and PG coatings on protein adsorption, blood coagulation and complement activation. Further, we investigated the anti-inflammatory capacity and the cytocompatibility of polyphenolic coatings in both human gingival fibroblasts (hGFs) and human whole blood to establish their potential for an improved wound healing around titanium implants.

2 | EXPERIMENTAL

2.1 | Materials

Details for the used materials and assays described in the experimental setups listed below are given in the ESI.

2.2 | Coating formation

Tannic acid and PG coating solutions were prepared at a concentration of 1 mg/ml. TA solutions contained 100 mM HEPES, 600 mM NaCl, 100 μ M Si_{aq} at either pH = 6.8 or pH = 7.8, to investigate the effect of a different coating thickness and chemistry.²⁷ PG solutions contained 100 mM HEPES, 100 mM MgCl₂ at pH = 7.0.²⁸ Grade IV titanium coins were aseptically coated in vials containing 10 ml of coating solution on a rocking platform at 30 rpm for 24 h (Figure S1). After the coating formation, the coins were washed and sonicated in sterile water to remove unbound molecules and precipitated particles. The coated surfaces are referred to as TA 68, TA 78, and PG 70 depending on the coating solution while the uncoated control surfaces are called Ti.

2.3 | Plasma and protein adsorption

Lyophilized citrated human plasma was reconstituted with water and diluted to 25% (v/v) in 10 mM phosphate buffer supplemented with 137 mM NaCl (PBS) at pH = 7.0. Fibrinogen, bovine serum albumin (BSA), and IgG were diluted in PBS at 200 μ g/ml. Adsorption was quantified using a quartz crystal microbalance with dissipation monitoring (QCM-D, QSense E4, BiolinScientific) under initial flow of 100 μ l/min for 5 min at 21°C, followed by monitoring of the adsorption at a flowrate of 10 μ l/min. Polyphenolic coatings were performed for 2 h and rinsed with PBS for 15 min before plasma and protein adsorption. The viscoelastic properties of the protein layer were modeled as described in the supporting information.

2.4 | Blood sampling and blood experiment design

Experiments with human blood were performed according to the ethical guidelines from the declaration of Helsinki with the approval of local ethical committee. Informed written consent was obtained from all blood donors. Blood from healthy human donors was obtained by forearm venipuncture using a 21-gauge needle. The whole blood (4.5 ml) was collected in polypropylene tubes containing 0.5 ml of 500 μ g/ml of the thrombin inhibitor lepirudin (Refludan[®], Celgene, Uxbridge, UK) as anticoagulant. Immediately after collection, an aliquot of 400 μ l of blood was taken and 64 μ l of a stop solution (CTAD solution [0.08 M trisodium citrate, 11 M theophylline, 2.6 M adenosine, 0.14 M dipyridamole] and 0.14 M

EDTA) was added to this aliquot. This blood sample was centrifuged at 3000 g for 30 min at 4°C. After centrifugation, plasma in the supernatant was collected and referred to as T_0 sample. Meanwhile, 400 μl of blood was incubated with one coin each of the different surfaces in a rolling incubator at 37°C. Depending on detection markers, as described below, an aliquot of incubated blood was taken at different time points. Blood was collected from three donors and experiments with blood from each donor was performed in triplicates ($n_e = 9$).

2.4.1 | Complement activation

After 30 min incubation, aliquots of 80 μl of incubated blood as described earlier were transferred into polypropylene vials containing 12.8 μl of the stop solution, followed by centrifugation at 3000 g for 30 min at 4°C. After centrifugation, plasma was collected and stored at -80°C for further analysis. Activation of the complement system was quantified by the level of its activation products C4d, and terminal C5b-9 complement complex or (TCC), using ELISA kits following the instruction provided by the manufacturer (see the ESI). The alternative pathway convertase, C3bBbP, was quantified using an in-house ELISA assay.²⁹ PBS and *Escherichia coli* ($10^7/\text{ml}$) were used as negative and positive controls, respectively.

2.4.2 | Coagulation activation

Activation of the coagulation system was quantified by the level of the thrombin activation markers thrombin-antithrombin complex (TAT) and prothrombin fragments F1 + 2 using ELISA kits following the instruction provided. Sample aliquots were taken 30 min after start of incubation, as described for the complement activation. PBS and *E. coli* ($10^8/\text{ml}$) were used as negative and positive controls, respectively.

2.4.3 | Platelet activation

After 30 min of incubation, 40 μl blood was taken to detect platelet activation. After adding 6.4 μl of the stop solution, the platelets were stained for 30 min in the dark at 4°C with CD42a-FITC, CD63-PE-Cy7, and CD62P-PE. After lysing red blood cell with a fixative-free lysis buffer (Introvigen™, Cat# HYL250), the platelets were resuspended and fixed in PBS containing 0.1% paraformaldehyde (PFA) and 0.1% bovine serum albumin (PBSA). Platelet activation was measured using an Attune NxT Acoustic Focusing Cytometer (Thermo Fisher Scientific). Platelets were gated as CD42a positive (CD42a+) population while their activation was measured by the expression of CD62P and CD63 markers on their surfaces. Data was analyzed with Flowjo software version 10.

2.4.4 | Granulocyte and monocyte activation

A 40 μl aliquot of incubated blood was taken after 30 min to quantify the activation of granulocytes and monocytes. After adding 6.4 μl of the stop solution, the cells were stained for 30 min in the dark at 4°C with CD45-Pacific Orange, CD14-PerCP, CD11b-APC/Fire 750, and CD35-Alexa Fluor 647. After lysing red blood cell with the fixative-free lysis buffer, the cells were resuspended and fixed in PBSA. The expression of abovementioned markers was analyzed with Attune NxT Acoustic Focusing Cytometer. Granulocytes were gated as the population positive for both CD45 and CD15 (CD45+/CD15+), while monocytes were gated as the population positive for both CD45 and CD14, but negative for CD15 (CD45+/CD14+/CD15-). The activation of granulocytes and monocytes was evaluated by the expression of CD11b and CD35.

2.4.5 | Cytokine profile

After 4 h incubation, 25.6 μl of the stop solution was added to remaining 160 μl incubated blood. Plasma collected after centrifugation was analyzed for the levels of a panel of 27 cytokines using a MAGPIX multiplex system (Bio-Rad Laboratories). The data were assessed by software optimized standard curves as generated using Human Standard I (Bio-Rad) supplied with the multiplex kit.

2.5 | Antioxidant capacity

2.5.1 | Dissolved polyphenolic molecules

The antioxidant capacity of polyphenolic molecules was quantified using the 2,2'-azino-bis(3-ethylbenzothiazoline-6-sulfonic acid (ABTS) assay.³⁰ 7 mM ABTS was mixed 1:1 with 2.45 mM $\text{K}_2(\text{SO}_4)_2$ and left to react overnight to create the ABTS^{•+} radical. The solution was diluted with MilliQ water to an adsorption value of 0.7 at $\lambda = 734 \text{ nm}$ (Lambda25, PerkinElmer, using a quartz cuvette with 10 mm path-length). Then 10 $\mu\text{l}/\text{ml}$ of polyphenol solution was added to the ABTS solution, and the mixture was vortexed for 1 min. The absorbance was then measured after 5 min. The trolox equivalent antioxidant capacity (TEAC) was calculated from a calibration curve.

2.5.2 | Antioxidant capacity of coatings

The antioxidant capacity of polyphenolic coatings was quantified using the ABTS assay adapted for a microplate reader. Briefly, ABTS solution was prepared as described above and the absorption was adjusted to 1.0 for 200 μl in a 96-well. Six coated Ti coins were incubated in ABTS solution at 1 ml/coin in the dark at room temperature (RT) with gentle shaking at 50 rpm. Then, 200 μl aliquots were taken at different time-points and the absorbance at $\lambda = 690 \text{ nm}$ was measured.

2.6 | Quantification of released polyphenols

The total dissolved polyphenol content was quantified using the Prussian Blue assay.³¹ In brief, MilliQ water was filtered thrice through activated charcoal to remove any iron contaminants. Six coated coins were incubated in filtered MilliQ water at 1 ml/coin at RT under gentle shaking at 50 rpm. Aliquots of 150 μ l were then transferred to a 96-well plate. To each well of 96-well plate, 25 μ l of 20 mM FeCl₃ dissolved in 0.1 M HCl was added, followed by 25 μ l of 16 mM K₄Fe(CN)₆. The color was left to develop for 5 min at RT under shaking before the absorbance at $\lambda = 690$ nm was measured. The concentration was calculated from a standard curve.

The release kinetics was quantified using a quartz crystal microbalance (QSense E4, BiolinScientific) in situ under constant flow of 100 μ l/min. After equilibration of Ti sensors (QSX310) in coating buffer, rinsing buffer (10 mM citrate/phosphate buffer, 137 mM NaCl) was flown to obtain the buffer-based change in frequency (ΔF) and dissipation (ΔD). TA and PG coatings were then deposited for 2 and 8 h, respectively. Before changing to rinsing buffer, the chamber was flushed with coating buffer to remove residual TA and PG molecules.

2.7 | hGF cell culture

Human gingival fibroblasts (hGFs; Provitro) were routinely cultured at 37°C/5% CO₂ in Dulbecco's modified Eagle's medium (DMEM), containing 4500 mg/ml glucose, 10% fetal bovine serum (FBS), 50 U/ml penicillin, 50 mg/ml streptomycin, and 2 mM GlutaMAX. Cells were subcultured before reaching confluence using trypsin/EDTA. Trypan blue stain was used to determine total and viable cell number. Cells were seeded at a density of 7×10^3 cells/well in 96-well plates, except for the comet assay (3.5×10^3 cells/well) and intracellular reactive oxygen quantification (25×10^3 cells/well in 48-well plate). Experiments were performed with cells at passages ≤ 8 after isolation.

2.7.1 | Induction of inflammation in hGFs

Following 2 h incubation at 37°C/5% CO₂ to allow cell adhesion, cells were washed with PBS and inflammation was induced by incubation in serum depleted medium containing 1% FBS, 1 μ g/ml *Porphyromonas gingivalis* derived LPS, and 1 ng/ml IL-1 β at 37°C/5% CO₂. LPS and IL-1 β were always freshly added to the medium. Optionally, cells were simultaneously treated with 25 μ g/ml TA or 5 μ g/ml PG.

2.7.2 | Confocal imaging

To assess cell morphology following induced inflammation for 48 h, the cells were carefully washed with PBS and fixed with 4% paraformaldehyde for 20 min at RT. Cells were stained with 5 μ g/ml Alexa Fluor 568 Phalloidin and 300 nM DAPI dissolved in PBS containing 0.2% Triton X-100 for 30 min at RT in the dark. Three non-

overlapping images were taken on two samples of each group using a Leica SP8 upright confocal laser scanning microscope with a 10 \times /0.40 HCPL APO CS objective.

2.8 | Cytotoxicity

Lactate dehydrogenase (LDH) activity was measured as an indicator for membrane-associated cell death. hGFs were incubated in 96-well plates. Then, 100 μ l of cell culture medium was collected after 24 h and mixed 1:1 with a reaction mixture according to manufacturer's instructions, and incubated at RT for 30 min. The oxidation of NADH was measured spectrophotometrically (ELx800, BioTek Instruments) at 490 nm. Results for test groups are calculated relative to a low control (C⁻, cells on tissue culture plastic [TCP]) and a high control (C⁺, cells on TCP with 1% Triton X-100) based on Equation (1):

$$\text{Cytotoxicity (\%)} = \frac{\text{Sample} - \text{C}^-}{\text{C}^+ - \text{C}^-} \times 100 \quad (\text{Equation 1})$$

2.9 | DNA damage

An alkaline comet assay was used to quantify permanent DNA damage in hGFs exposed to the polyphenolic molecules as described in the supplementary information. Cells in H₂O₂-treated sample groups were exposed to 50 μ M H₂O₂ for 4 h prior to sample collection. Nuclei were stained with SYBR gold at RT for 15 min in the dark shortly before imaging. Slides were imaged using a fluorescence microscope with 4 \times objective (Olympus IX70). At least 100 nuclei per sample were imaged and analyzed using the OpenComet plugin for ImageJ.

2.10 | Intracellular reactive oxygen

hGFs were seeded on coated Ti coins, placed in a 48-microwell plate, and incubated over-night at 37°C/5% CO₂ in complete medium to avoid any additional oxidative stress.³² hGFs seeded on TCP served as control. One hour before inducing inflammation, 2.5 mM N-acetyl cysteine (NAC) or dissolved polyphenolic molecules (25 μ g/ml TA; 5 μ g/ml PG) were added to the cell medium. Subsequently, inflammation was induced by replacing the cell medium with 300 μ l fresh medium containing LPS/IL-1 β as described above. Alternatively, 200 μ M tert-butyl hydroperoxide (TBHP) was added to the incubation medium. Following a 1 h incubation period, 2 μ M CellROX DeepRed stain was added and the cells were incubated for another hour. Live/dead staining was performed with 500 nM PI for 15 min in the dark. All concentrations are given as final concentrations per well content.

To assess intracellular ROS by flow cytometry, cells were trypsinized and resuspended in PBSA. The flow cytometer (Attune NxT, Thermo Fisher Scientific) was calibrated with unstained cells,

CellROX DeepRed stained TBHP treated cells, and PI-stained Triton X-100 permeabilized cells. At least 20,000 events were registered and gated as described in Figure S2. For all groups physical duplicates ($n_e = 2$) were analyzed.

2.11 | Inflammatory response

Multianalyte profiling was performed to measure inflammatory markers secreted in cell culture medium from hGFs at 6, 24, and 48 h after induced inflammation using a Luminex 200 system. Median fluorescent intensity was analyzed using a 5-parameter logistic line-curve fitting method for calculating analyte concentrations in samples via the xPONENT 3.1 software (Luminex). Levels of interleukin-6 (IL-6), interleukin-8 (IL-8), monocyte chemoattractant protein-1 (MCP-1), and tumor necrosis factor alpha (TNF- α) were measured using Human Cytokine/Chemokine Magnetic Bead Panel kit. The assay was performed according to the protocol provided by the manufacturer.

Total and phosphorylated (pS536) NF- κ B p65 levels in hGFs were determined 0.5 h after induced inflammation using the respective Human InstantOne™ ELISA kits (Invitrogen) according to the protocol provided by the manufacturer.

2.12 | Statistical analysis

Data was evaluated for statistical significance using ANOVA (RStudio 1.4). Data was checked for normality using Shapiro–Wilk test and homogeneity of variances by Levene test. The ANOVA test included Ti, TA 68, TA 78, and PG 70 sample groups.

3 | RESULTS AND DISCUSSION

3.1 | Blood plasma and protein adsorption

Protein adsorption onto a surface determines its subsequent recognition and response by the host immune and hemostatic systems. Primarily, fibrinogen from blood plasma is found to deposit on oxide surfaces,³³ promoting subsequent platelet adhesion. Deposited fibrinogen is then replaced by higher molecular weight proteins during prolonged exposure to blood.³⁴ Therefore, it is important to investigate whether surface modifications cause a change in plasma protein adsorption on the implant surface. Further, the chemical and topographical properties of surfaces are influencing factors of the protein adsorption. Polyphenolic coatings such as investigated in this study have a roughness of approximately 11 nm, are hydrophilic and have negative zeta potential.^{27,35,36}

The total amount of plasma proteins absorbed on TA coatings was higher than those on PG coatings and bare Ti surfaces, as quantified by QCM-D (Figure 1A). The protein layer formed on both TA surfaces also showed a higher viscosity and elastic modulus resulting in a more rigid protein film structure as indicated by the lower loss tangent

(G''/G') (Figures 1B and S3). $\Delta D/\Delta F$ plots further attested different adsorption profiles of plasma proteins on the different surfaces (Figure S4). Together, these changes indicate a difference in the structure of the protein layer absorbed on each surface. Upon rinsing the protein layer with PBS, loosely bound proteins in the outer layers desorbed, as evidenced by a reduction in mass (Figure 1A). After the rinsing step, the viscosity of the protein layers was equal for all four studied surfaces, whereas the elastic modulus differed (Figure S3). Thus, the structural differences persisted even after desorption of the loosely attached proteins.

Due to the complexity in protein composition of human plasma, we further studied single protein adsorption of three abundant plasma proteins albumin, fibrinogen, and IgG. Albumin is the most abundant protein in plasma and governs the initial adsorption of plasma proteins on surfaces.³⁷ However, albumin is later displaced by other proteins with higher affinity to the surface.³⁷ Albumin formed a thin rigid layer on Ti, TA 78, and PG 70 coatings while a more dissipative structure was observed on TA 68 coatings (Figure 1B). At physiological pH, albumin adsorbs on SiO₂ and TiO₂ surfaces in its native conformation via electrostatic interaction and hydrogen bonding.³⁸ Because the adsorption characteristics on Ti and PG 70 coatings were comparable to the adsorption on TiO₂ (Figure S5),³⁹ we assume that albumin adsorbed in its native α -helical state.⁴⁰ The increase in dissipation observed on TA coatings may be due to potential hydrophobic interactions and hydrogen bonding of albumin with polyphenolic molecules, leading to its denaturation.⁴⁰ Rinsing with PBS did not cause desorption from any of the tested surfaces, suggesting that the protein layer was stable in the absence of competitive adsorption.

Fibrinogen is a key component of the coagulation cascade and its adsorption onto a surface affects the adhesion of platelets.⁴¹ Particularly the change in conformation and loss of its native α -helical structure is correlated to increased platelet adhesion.⁴² Thus, we next investigated the adsorption of fibrinogen and observed a similar trend as with albumin and plasma. TA 68 and TA 78 surfaces showed an increase in fibrinogen adsorption compared to Ti and PG 70 (Figure 1A). Further, the fibrinogen layer was more rigid on TA modified surfaces (Figure 1B). Upon rinsing with PBS, the amount of fibrinogen remained unchanged, indicating a tightly bound layer. Fibrinogen showed a high binding affinity to Ti, which was even increased on TA functionalized surfaces (Figure S6). However, the splitting harmonics suggested a structural change within the formed layer on TA 68 and TA 78. This could be due to the changes in internal structure of fibrinogen. A study by Yang et al. showed that the conformation of fibrinogen upon adsorption onto polyphenolic surfaces was dependent on interactions with galloyl groups.⁴³ Increasing number of galloyl groups decreased the γ -chain activity of fibrinogen resulting in less platelet adhesion. Our results were also in good agreement with a study by Tardy et al., which showed a higher amount of fibrinogen deposition on TA/Fe³⁺ multilayers compared to albumin and plasma.⁴⁴

Last, we studied the adsorption of the plasma protein IgG. When bound to a surface, IgG can bind C1q and activate the classical complement pathway.⁴⁵ Similar to the other proteins studied previously, Ti and PG 70 resulted in similar IgG adsorption, whereas TA coatings

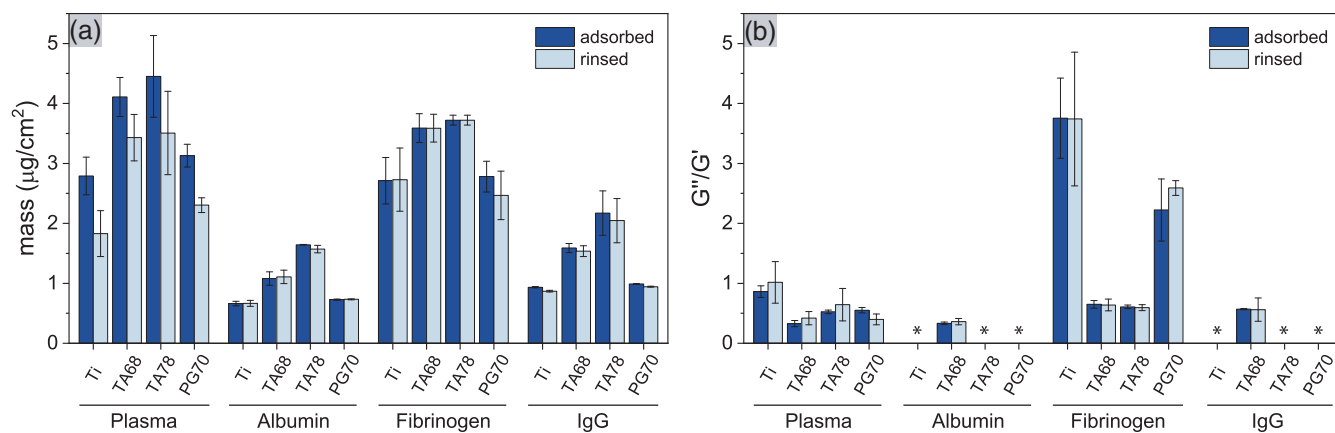


FIGURE 1 Adsorption of plasma proteins on Ti surfaces and pyrogallol (PG)- and tannic acid (TA)-coated Ti surfaces as quantified by quartz crystal microbalance with dissipation monitoring (QCM-D). (A) Adsorbed mass and (B) viscoelastic properties of citrate-anticoagulated plasma. Plasma was diluted to 25% (v/v) in phosphate buffered saline (PBS). The amount of the three abundant plasma proteins, albumin (67 kDa), fibrinogen (340 kDa), and IgG (150 kDa), was selectively quantified at their incubation concentrations of 200 µg/ml. Polyphenolic coatings were obtained for 2 h prior to plasma protein adsorption. Four individual adsorption curves were monitored and values are given before and after rinsing with PBS ($n_e = 4$). (*) Rigid layers where modeling failed. Data are presented as mean \pm SD

resulted in a higher surface coverage of IgG (Figure 1A). While the initial IgG adsorption was more rapid on all polyphenolic coatings (Figure S7), TA 68 modified surfaces resulted in a less rigid protein layer compared to the other surfaces (Figure 1B). Splitting harmonics suggested a change in internal layer structure especially on TA 68 coatings (Figure S7). In practice, a low adsorption of IgG may be beneficial since *in vivo* studies have shown that IgG-modified implants recruited more leukocytes.^{46,47} Thereby, the inflammatory response caused by the IgG-modified Ti implants delayed the early tissue integration of the modified implants.

Although we observed a clear difference in blood plasma adsorption onto the different polyphenol-coated surfaces, the impact on the level of individual proteins remains complex. The potential inhibition of protein rearrangement may further impact the adsorption and conformation of complement and coagulation components.

3.2 | Interactions with human whole blood

To evaluate whether polyphenolic coatings can modulate inflammatory or thrombotic responses after the implant placement, we explored the interactions of whole blood with our surface coatings. Since polyphenols, such as TA, interact with blood components,⁴⁸ we focused on the activation of the complement and coagulation system. These two systems largely determine whether the surface is accepted by the host upon implantation.⁴⁹

3.2.1 | Complement activation

The complement system is one of the key components of innate immunity and can be activated via three pathways: the classical, the

lectin, and the alternative pathway.⁵⁰ Along the activation cascade, different activation products are generated, which in turn play pleiotropic functions in immune responses.⁵¹ Many of these products can be used as activation markers. C4d is an activation product common for both the classical and the lectin pathway.⁵⁰ It was detected at elevated levels on all surfaces, implying the activation of either or both of these pathways (Figure 2A). C3bBbP is the C3-convertase of the alternative pathway of the complement system.⁵⁰ The formation of C3bBbP complex was found in blood samples incubated with all surfaces, suggesting the activation of the alternative pathway (Figure 2B). This is in agreement with known activation of the alternative pathway on surfaces bearing nucleophiles, such as polyphenolic hydroxyl groups, and on protein layer formed on surfaces.^{52,53} Regardless of the activation, all pathways of the complement system converge at the central C3 and C5 proteins, and subsequently combine with C6–C9 to form termination complement complex or TCC.⁵⁰ Although elevated levels of C4d and C3bBbP were detected for all surfaces compared to negative control (C–), polyphenolic coatings did not induce increased levels of TCC (Figure 2C). While Ti surfaces yielded low TCC levels compared to the positive control, TA and PG coatings maintained TCC concentrations on the level of C–. These results suggest that the modified surfaces may inhibit the further amplification process of the complement cascade and reduce the release of C3a and C5a.

3.2.2 | Coagulation activation

The coagulation system has a critical role in hemostasis.⁵⁴ It can be activated through two pathways, intrinsic and extrinsic, generating functional activation products along these two cascades.⁵⁵ Ti surfaces induced high levels of both TAT and F1 + 2 (Figure 2D,E). As products

from thrombin activation, they mark the activation of coagulation. This is in accordance with a previous study showing the induction of blood coagulation by Ti surfaces.⁵⁶ Both TA 68 and TA 78 modified surfaces had lower TAT levels, but TA 78 induced an increase in F1 + 2 (Figure 2D,E). TAT and F1 + 2 levels for PG surfaces were comparable to Ti surfaces within the margin of error. These results confirm a previous study where low amount of TA did not affect the coagulation of blood.⁵⁷ Extrinsic activation of the coagulation system by implant surfaces is known to be dependent on surface charge and hydrophobicity.^{58,59} Our results showed that the coated surfaces maintain the thrombogenic activities of bare Ti surfaces, despite their altered surface chemistry. This may also preserve the osseointegrative property of Ti, which is linked to a thrombin stimulated osteoblast proliferation.⁶⁰

3.2.3 | Platelet activation

Platelets play a vital role in hemostasis and inflammation.⁶¹ Their activation is closely connected to both the complement and the coagulation system.⁶² To evaluate whether different surface coatings elicit platelet activation, we measured the expression of two surface activation markers, CD62P and CD63, using flow cytometry. Upon activation, CD62P (P-selectin) rapidly mobilize from α -granules to the platelet surface, by which it can mediate the binding of platelets to cells expressing P-selectin glycoprotein ligand-1 (PSGL-1).⁶³ Expression levels of CD62P increased after incubation with all surfaces, implying platelet activation (Figure 3A). In contrast, CD63 is not associated with platelet adhesion, but mediates platelet spreading and aggregation. CD63 expression remained as low as observed in both T₀ and C-, suggesting that different coatings did not induce a significant change in platelet morphology (Figure 3A). CD62P and CD63 expression together indicated that all different surfaces induced an early activation of platelets, but not a significant change in their aggregation

3.2.4 | Monocyte and granulocyte activation

Activation of monocytes and granulocytes is a hallmark for acute inflammation. Both activation markers CD11b (macrophage-1 antigen) and CD35 (complement receptor 1) remained unchanged at the background level observed in the negative control (Figure 3B,C). The expression of both CD11b and CD35 is closely linked to the activation of the complement and coagulation systems.⁵¹ Combined with the results described earlier (Figure 2), these results imply that although different surface coatings induced the activation of these two systems, the activation was not sufficient to elicit significant cellular responses against these surfaces.

3.2.5 | Cytokine profile

A panel of 27 plasma cytokines was analyzed after incubation with different coating surfaces. Six cytokines most relevant for

inflammation are presented in Figure 4. In general, TA-coated surfaces did not induce a significant change in expression of any cytokines while PG-coated upregulated leukocyte chemotactic cytokines (Figures 4 and S8). Upregulation of IL-8, a vital chemoattractant for leukocyte recruitment,⁶⁴ has previously been found after incubation of neutrophils with penta-galloyl glucose (PGG).⁶⁵ Thereby, the wound healing process may be supported by reducing the pro-inflammatory reaction of neutrophils.

3.3 | Antioxidant capacity

Dissolved polyphenols are generally considered as antioxidant molecules with a structure-dependent capacity to scavenge free radicals.¹³ Thus, we investigated the antioxidant capacity of our molecules and whether the antioxidant properties of TA and PG are conserved when deposited on Ti surfaces. As shown in Figure 5A, PG and gallic acid (GA) showed a 4-times higher antioxidant capacity compared to trolox. GA is the structural subunit of TA, which can consist of up to 10 GA units. TA reached a TEAC value of 16 (Figure 5A). This corresponds to four GA units and may suggest that either only the outer GA groups in TA are active in scavenging radicals, or that commercial TA has a high degree of fragmentation. The latter assumption is supported by the evidence of a high GA content in commercial TA.⁶⁶ As the radical formation of polyphenols is pH dependent,⁶⁶ we observed a peak in TEAC for TA at pH = 7 before a reduction in TEAC occurred with increasing pH (Figure S9A). This behavior was not observed for PG and can be explained by the onset of oxidation for TA at pH = 7, whereas PG oxidizes already at lower pH (Figure S10). Upon oxidation with NaMnO₄, the TEAC of TA showed the same behavior, indicating the impact of the oxidation state of the molecule on its radical scavenging capacity (Figure S9B). In the subsequent analysis of the TEAC of TA and PG coatings, we observed that modified surfaces rapidly discolored ABTS solutions (Figure 5B). To investigate whether this was an effect of released or surface-confined molecules, we quantified the amount of polyphenolic molecules released from the surface. TA 68 coatings showed the highest amount of released molecules with 13 μ g/ml, which corresponds to 7.6 μ M TA, while TA 78 and PG 70 surfaces released only 8.5 μ g/ml (5 μ M TA) and 2.5 μ g/ml (20 μ M PG) (Figure 5C). This can be attributed to the larger thickness of TA 68 coatings compared to TA 78 and PG 70 coatings.^{27,28} However, the full reduction of the ABTS solution by the coatings indicated a calculated concentration of more than 10 μ M (17 μ g/ml) of TA and 30 μ M (4 μ g/ml) of PG. Thus, not only the released molecules were responsible for the observed antioxidant effect, but also the active surfaces. The released amount of TA molecules further confirms that the concentration is below the threshold where adverse effects with blood were observed.⁴⁸

TA coatings disassemble in strong acidic and alkaline condition.²⁷ Since inflammation can cause local acidosis,⁶⁷ we further investigated the release of molecules at various pH levels. The dissolution kinetics of TA and PG coatings confirmed an initial burst release of molecules as shown in Figure 5C, which tapered off after 4 h (Figure S11A). The

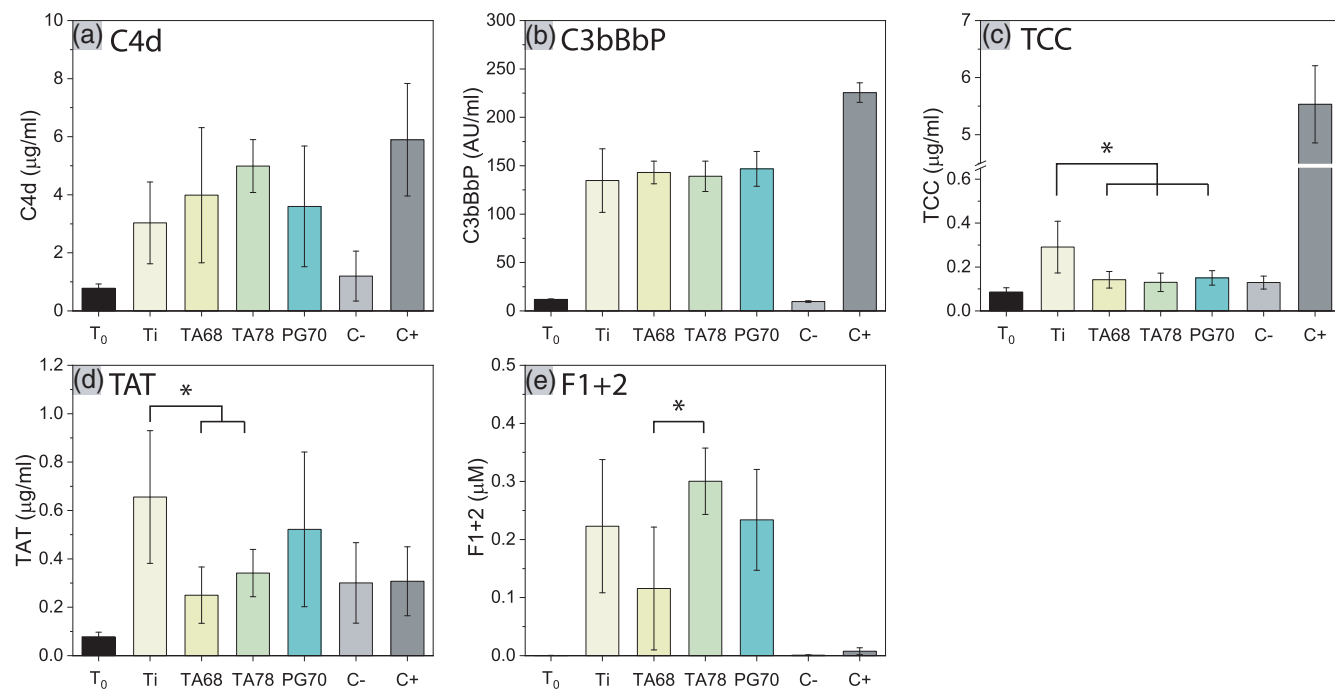


FIGURE 2 Interaction of different surface coatings with human whole blood. Markers of (A–C) complement activation and (D, E) coagulation activation after 30 min incubation of human whole blood with Ti, pyrogallol (PG)-, and tannic acid (TA)-coated surfaces at 37°C. T₀ refers to the blood sample before incubation and serves as baseline levels. C- and C+ are negative and positive controls with blood without any activator and blood incubated with *Escherichia coli*. Blood was taken from three donors and three samples per group were analyzed ($n_e = 9$). Values represent mean \pm SD. (*) p value < .05

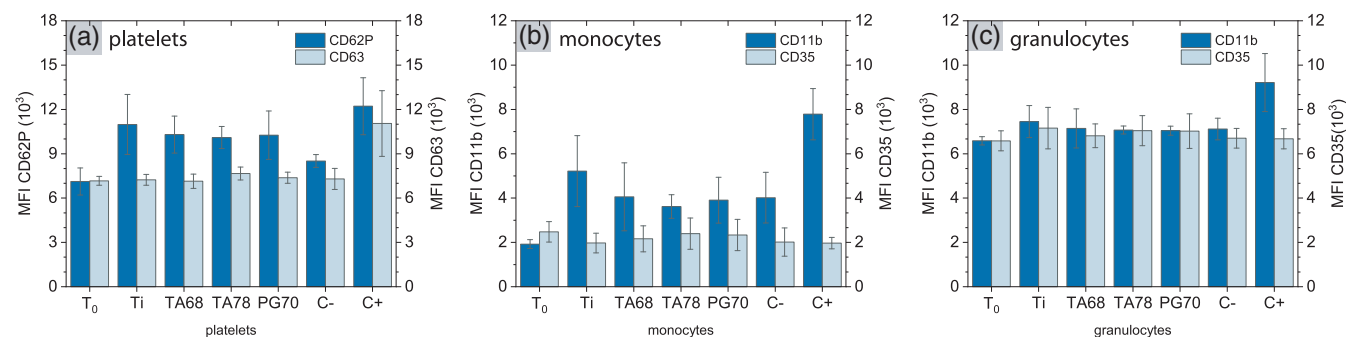


FIGURE 3 Activation of platelets, monocytes, and granulocytes. Blood was incubated with Ti, pyrogallol (PG)-, and tannic acid (TA)-coated surfaces for 30 min. (A) The activation of platelets was quantified by the expression levels of CD62P and CD63 using flow cytometry. The activation of (B) monocytes and (C) granulocytes was measured by the levels of CD11b and CD35. Experiments were conducted in triplicate with blood from three donors each ($n_e = 9$). Results are presented as median fluorescent intensity (MFI) \pm SD. No statistical significance was obtained

least reduction of the polyphenolic layer mass was observed at neutral pH (Table S1). Either increasing or decreasing the pH resulted in a higher release of the layers. At pH = 3, TA coatings rapidly dissolved within 2 h whereas PG coatings remained more stable (Figure S11B).

Cell culture medium is an additional factor influencing the release of polyphenols in cell experiments. We attempted to quantify the release of polyphenols in DMEM, but simultaneous protein adsorption onto TA and PG coated surfaces made it unfeasible (Figure S12). Although the release in medium could not be directly measured, we expect that some molecules are being released to provide an antioxidant effect.

3.4 | Cytotoxic effect on hGFs

Ti is a remarkable material for bone implants.⁶⁸ However, improvement of soft tissue integration is often neglected. Soft tissue integration plays an important role for dental implants, where fibroblasts are responsible for remodeling granular tissue and provide a close seal of the gingiva to protect the implant surface from the oral environment.⁶⁹ Hence, we proceeded to explore whether PG and TA coatings affect the response of hGFs under inflammatory conditions.

LDH assay showed low level of cytotoxicity towards hGFs for TA concentrations up to 250 μg/ml, whereas PG concentrations above

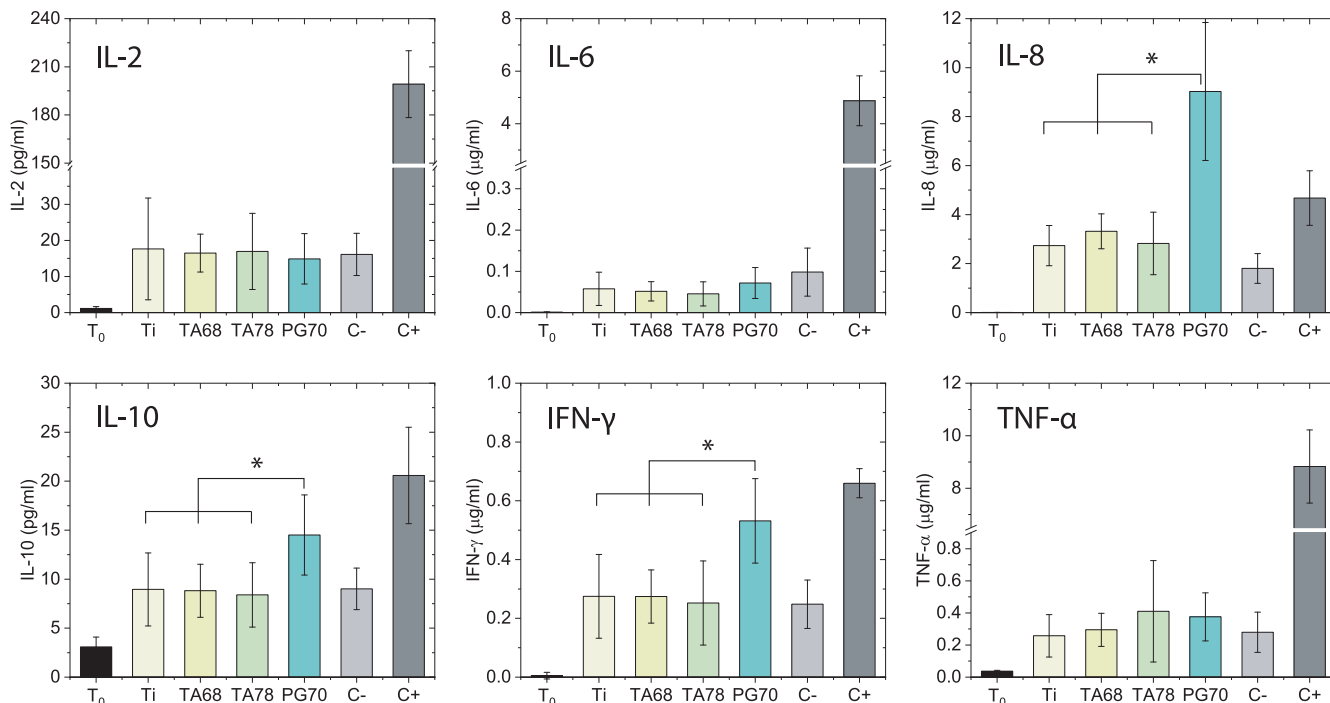


FIGURE 4 Expression profile of selected plasma cytokines. Plasma cytokines were measured after 4 h incubation of blood with Ti, tannic acid (TA)- and pyrogallol (PG)-modified surfaces. Experiments were conducted in triplicates with blood from three donors each ($n_e = 9$). Results are presented as mean \pm SD. Data for other cytokines are presented in Figure S8. (*) p value < .05

5 $\mu\text{g/ml}$ showed considerable cytotoxic effect (Figure 6A). The higher apparent cytotoxic effect can be explained by the 10 times higher molar concentration of PG compared to TA. hGFs seeded on either TA or PG coatings showed low cytotoxicity (Figure 6B), which was consistent with the low non-toxic concentrations of TA and PG released from the coatings (Figure 5C). Furthermore, cells spread and adopted the typical spindle-shaped cell morphology of healthy fibroblasts on all tested surfaces (Figure S13), which correlates with the obtained LDH results.

These results show that the coatings did not influence the integrity of hGFs cell membrane. However, polyphenolic compounds and their oxidation products, quinones, are potentially mutagenic agents.⁷⁰ In addition to their antioxidant effect, polyphenols may also elicit pro-oxidant properties, such as the production of ROS, which may lead to DNA damage and apoptosis.^{71–73} Indeed, both TA 78 and PG 70 coatings showed higher DNA damage compared to bare Ti surfaces (Figure 6C). While the DNA damage caused by dissolved TA was slightly higher compared to the TA coating, dissolved PG did not induce more DNA damage than Ti. The high DNA damage caused by coatings could be an effect of the concentration of the released molecules in the working volume of the assay but cannot be correlated with cytotoxic effects (Figure 6A). Interestingly, both dissolved PG and PG coatings reduced the DNA damage induced by 50 μM H_2O_2 compared to the negative control (TCP). In contrast, TA caused higher DNA damage in combination with H_2O_2 (Figure 6C).

The mutagenicity and toxicity of polyphenols can occur through either coupling of the highly reactive phenolic compounds to cell

components (arylation) or redox reactions creating reactive radical species.⁷⁴ Once polyphenolic compounds are oxidized to quinones, mutagenic effects have been shown to occur through electrophilic coupling reactions.⁷⁵ This pro-oxidant effect has been observed for GA in the absence of H_2O_2 .⁷² Since TA is a hydrolysable molecule, its degradation can yield GA. Such degradation processes have been observed in DMEM, where the resulting GA formed ROS and inhibited cell growth.⁷⁶ This means that in vitro studies are highly dependent on the culture conditions and the concentration of the polyphenols.

3.5 | Intracellular reactive oxygen species

Cells can be subject to oxidative stress caused by the release of reactive oxygen species (ROS) during inflammation. First, we investigated whether the inflammatory response of hGFs induced by LPS/IL-1 β is connected to intracellular ROS. CellROX staining showed no detectable level of intracellular ROS in hGFs (Figure 7A). The inflamed positive controls on TCP (C+) and Ti coin (Ti+) showed almost the same signal as the negative controls C- and Ti- that were not exposed to LPS/IL-1 β . All groups showed an unspecific CellROX signal intensity compared to the unstained control (US). Although ROS is often associated with phagocytes,⁷⁷ exposing fibroblasts to *P. gingivalis*-derived LPS and IL-1 has also resulted in elevated mitochondrial ROS expression.^{78,79} Our negative results could be an effect of the specific primary cells we used in this study. We observed that our hGFs did not

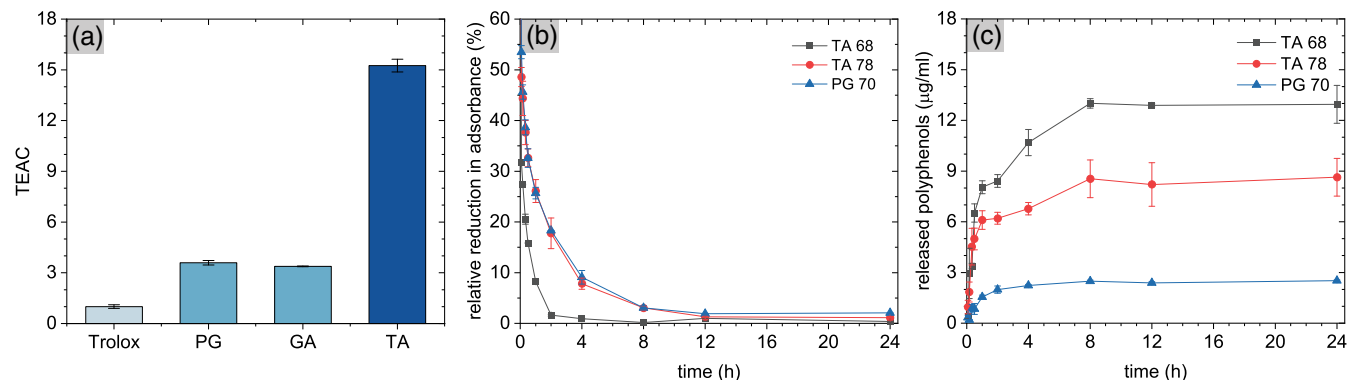


FIGURE 5 Antioxidant capacity of tannic acid (TA)- and pyrogallol (PG)-coated surfaces. (A) Trolox equivalent antioxidant capacity (TEAC) of polyphenolic molecules dissolved in water measured after 6 min ($n_e = 3$). (B) Absorbance reduction of 2,2'-azino-bis(3-ethylbenzothiazoline-6-sulfonic acid (ABTS) in presence of coated coins. (C) Release of polyphenolic molecules from one coated coin per 1 ml water. Results are presented as mean \pm SD

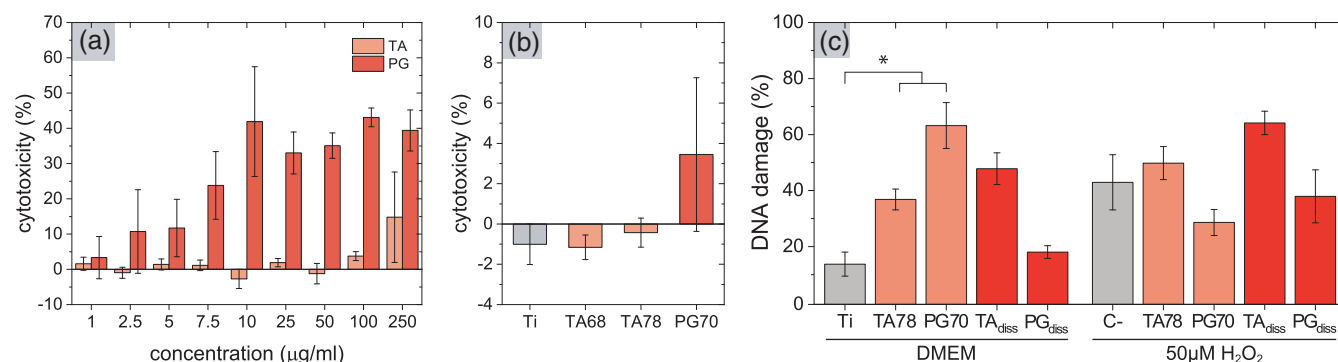


FIGURE 6 Cytotoxicity of tannic acid (TA) and pyrogallol (PG) on human gingival fibroblasts (hGFs). Cytotoxicity of (A) dissolved polyphenols ($n_e = 6$) and (B) polyphenolic-coated surfaces on hGFs as quantified by lactate dehydrogenase (LDH) assay ($n_e = 3$). (C) DNA damage of hGFs in presence of dissolved polyphenolic molecules (100 µg/ml TA, 5 µg/ml PG) or polyphenol-coated surfaces ($n_e = 6$). hGFs were cultured in complete medium or in the presence of H₂O₂. Note that the relative concentration of released TA and PG from coins (Figure 5C) into the medium (panel B) is potentially higher than direct supplementation (panel A) due to the working volume of 200 µl per well. Results are presented as mean \pm SD. (*) p value < .05

show an inflammatory response after LPS stimulation (Figure S14), and under certain circumstances, hGFs exposed to LPS can respond with LPS tolerance.⁸⁰

Besides endogenous ROS production, oxidative stress in hGFs can also be induced externally. During inflammation, recruited granulocytes and macrophages produce ROS, such as H₂O₂, to remove foreign objects by phagocytosis.⁸¹ ROS, which are able to cross cell membranes,⁸² can then induce oxidative stress and apoptosis in the surrounding cells.⁸³ Upon exposing hGFs to TBHP, dissolved TA reduced the intracellular ROS level close to that of the negative control (Figure 7B,C), demonstrating the high antioxidant capacity of TA. Despite its lower concentration, TA outperformed the higher concentrated antioxidant N-acetyl cysteine in reducing intracellular ROS upon TBHP stimulation. Dissolved PG also reduced the ROS level, which is in correlation with its TEAC (Figure 5A). Importantly, we also observed a reduction of intracellular ROS levels for hGFs cultured on coated TA and PG coins. Of the tested surfaces, TA 68 was found to be most effective in reducing intracellular ROS, probably due to the

higher number of molecules being released from the surface (Figure 5C) or the non-oxidized nature of the molecule. Both possibilities are plausible and in accordance with literature as well as our own results attesting decreased radical scavenging capacity of oxidized polyphenols (Figure S9).⁸⁴ None of the groups showed cytotoxic effects during TBHP treatment as determined by PI staining (Figure S15), which supports our LDH assays (Figure 6B).

In comparison to our DNA-damage results, which indicated that polyphenols can be pro-oxidant, ROS determination by flow cytometry did not indicate redox cycling in the presence of TBHP (Figure 7B). Correlation of DNA damage and intracellular reactive oxygen thus needs further research. However, the experiment verified that TA and PG coatings maintain their antioxidant properties in DMEM, despite protein adsorption on the coating surface (Figure S12). Thus, potential reaction of polyphenols with proteins through addition-reactions did not inhibit the radical scavenging properties of the molecules, which agrees with previous studies.^{85,86}

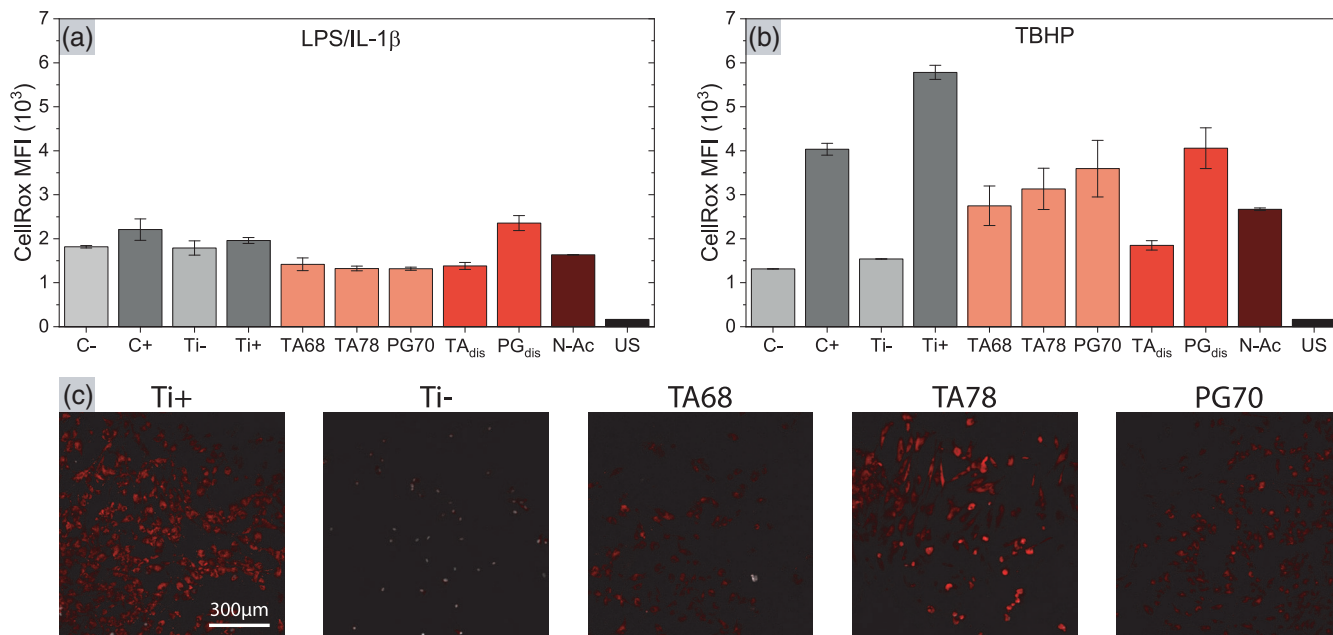


FIGURE 7 Intracellular reactive oxygen species (ROS) level. (A) CellROX intensity in human gingival fibroblasts (hGFs) after (bacteria derived) lipopolysaccharide (LPS)/IL-1 β induced inflammation as determined by flow cytometry. (B) Intracellular ROS levels in hGFs after exposure to 200 μ M tert-butyl hydroperoxide (TBHP). In both experiments, hGFs were inflamed for 2 h. CellROX DeepRed was added after 1 h. Concentrations for dissolved polyphenols were 250 μ g/ml TA and 5 μ g/ml pyrogallol (PG). 10 k cells were registered for two individual runs ($n_e = 2$) and results are presented as mean \pm SD. (C) Representative images show the intracellular ROS in hGFs inflamed by TBHP

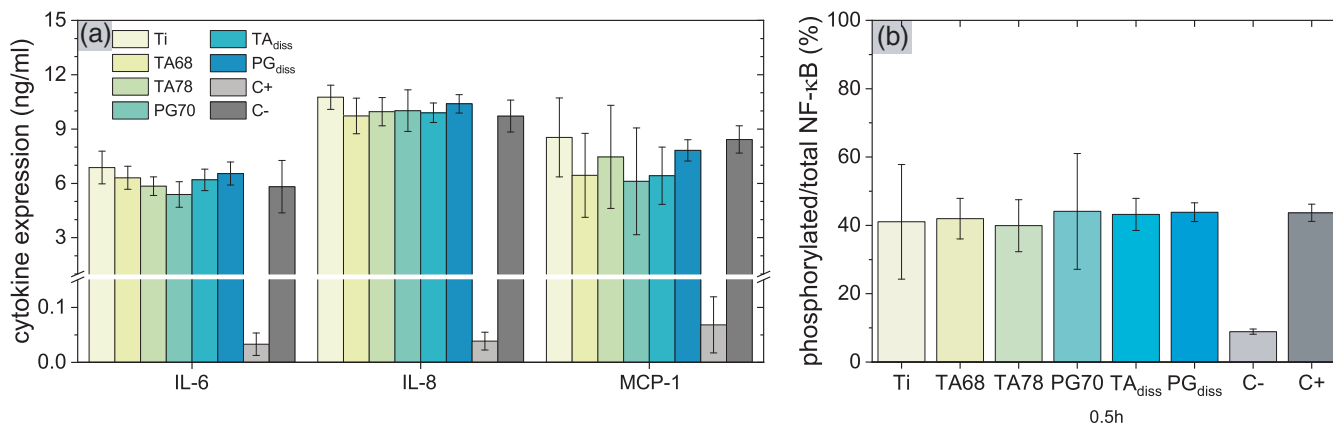


FIGURE 8 Cytokine expression and For Peer Review NF- κ B activation in human gingival fibroblasts (hGFs). (A) Multiplex analysis of inflammatory cytokine expression in hGFs 24 h after inflammation with (bacteria derived) lipopolysaccharide (LPS) and IL-1 β ($n_e = 6$). (B) Ratio of phosphorylated to total NF- κ B p65 in hGFs 0.5 h after inflammation by LPS and IL-1 β ($n_e = 3$). Concentrations for dissolved polyphenols were 250 μ g/ml TA and 5 μ g/ml pyrogallol (PG). Individual values for total and phosphorylated NF- κ B p65 are given in Figure S16D. Results are presented as mean \pm SD. No statistical significance was obtained

3.6 | Cytokine expression and regulatory effect of polyphenols

After detecting no ROS in LPS/IL-1 β stimulated hGFs, we continued to assess the expression of inflammatory cytokines. On Ti surfaces hGFs showed high levels of IL-6, IL-8, and MCP-1 (Figure 8A). This is in good relation with reported response of hGFs to IL-1 β and LPS derived from *P. gingivalis*.^{87,88} TNF- α levels were below the detection limit and thus not shown. Neither dissolved polyphenols nor the

modified surfaces affected the inflammatory response 24 h after stimulation with LPS/IL-1 β (Figure 8A). Similar observation was made 6 and 48 h after inducing inflammation (Figure S16).

Contrary to our results, other studies have found that TA and PG reduced the expression of pro-inflammatory cytokines in various human cells stimulated by LPS.⁸⁹⁻⁹¹ Further, several other polyphenolic molecules have been shown to reduce the inflammatory response in hGFs after stimulation with LPS.^{18,92,93} However, in our study, the inflammatory trigger was rather IL-1 β than LPS, as no inflammatory

stimulus was observed for LPS alone (Figure S14). Under stimulation with IL-1 β , polyphenols may not be able to curb the inflammatory cell response, as also suggested by a study using quercetin coatings.⁹⁴

Since the expression of the pro-inflammatory cytokines upon exposure to LPS and IL-1 β has been associated with NF- κ B signaling pathways,^{95,96} we investigated whether TA and PG affect NF- κ B signal transduction. We found equal level of phosphorylation of NF- κ B p65 in hGFs for all tested samples 30 min after induction of inflammation (Figure 8B). Contrary to previous studies,^{17,92,95–97} dissolved TA and PG did not reduce NF- κ B phosphorylation, which clearly correlated with the cytokine expression. We assume that our coatings could not inhibit the inflammatory response either due to the hGFs we used, or due to a low concentration of released polyphenols. Furthermore, other inflammatory signaling pathways besides NF- κ B p65 signaling should be considered, such as P13-K, MAPK, ERK, and p53.^{98,99} Thus, further studies need to be conducted to reliably discern the effect of the simultaneous induction of inflammation by LPS and IL-1 β and to investigate the dose-dependent effect of polyphenolic treatments in hGFs.

3.7 | Significance of the results on early wound healing processes

Protein adsorption is a key factor in the foreign body response. Polyphenolic coatings did not significantly change the amount of adsorbed proteins. Although the coatings activated the coagulation and complement system, we did observe statistically significant reduced levels of TCC. This may indicate a lower inflammatory response compared to bare Ti surfaces. Further, no upregulation in pro-inflammatory cytokines confirmed that our coatings did not stimulate inflammation. Regarding the anti-inflammatory effect, we observed reduced levels of intracellular ROS in hGFs cultured on coated surfaces. These results suggest that nonspecific oxidative stress caused by immune cells towards other cells can be reduced during the early wound healing process. However, inflammation in hGFs induced by LPS/IL-1 β could not be curbed. These cells were chosen to particularly study the healing of soft tissue around dental implants, as they are the first cells to arrive at the wound site after blood cells to remodel the blood clot.⁶⁹ In addition to hGFs, future research should evaluate the effect of polyphenolic coatings on other cell types, particularly immune cells such as macrophages,¹⁰⁰ before a more general conclusion can be drawn. Regarding other types of Ti implants, the respective cell types that are in primary contact with the implant need to be studied as well. Together, these experiments will then lay the foundation for further research that addresses the complex foreign body response in appropriate in vivo models.

4 | CONCLUSIONS

In this study, we investigated the effect of TA and PG coatings on the early wound healing processes and cell response under inflammatory

conditions. The polyphenolic surface modifications altered the initial blood protein layer formed on the surfaces, which is a key factor in the subsequent complement, coagulation, and platelet activation as well as cell adhesion. TA coatings generally showed higher protein adsorption compared to PG and Ti. Further, TA and PG coatings activated the classical, lectin, and alternative complement pathways like Ti surfaces. However, the formation of the terminal complement complex was reduced on the TA and PG coated surfaces. The thrombogenic properties of Ti were retained and high levels of TAT and F1 + 2 were found for TA and PG coated surfaces. This was corroborated by platelet activation. In contrast, monocytes and granulocytes were not activated by Ti or polyphenolic coatings, which was represented in the cytokine expression.

The modified surfaces showed antioxidant properties, which reduced intracellular reactive oxygen levels in hGFs. While the coatings showed good cytocompatibility, potential increase in DNA damage was observed. Upon inflammation of hGFs with LPS/IL-1 β , polyphenolic coatings were not able to reduce the expression of pro-inflammatory cytokines. This was linked to the activation of the NF- κ B p65 signaling pathway. Since inflammatory responses and signaling pathways are complex cell specific processes, further studies are needed to evaluate the ability of polyphenolic surface modifications to support early wound healing processes.

ACKNOWLEDGMENTS

This work was financially supported by the Research Council of Norway, grant number 302590 and 274332. The graphical abstract uses elements from Servier Medical Art, licensed under the Creative Commons Attribution 3.0.

CONFLICT OF INTEREST

The authors declare no conflict of interest.

DATA AVAILABILITY STATEMENT

Data available on request from the authors.

ORCID

Hanna Tiainen  <https://orcid.org/0000-0003-2757-6213>

REFERENCES

1. Ratner BD. In: Brunette DM, Tengvall P, Textor M, Thomsen P, eds. *Titanium in Medicine: Material Science, Surface Science, Engineering, Biological Responses and Medical Applications*. Springer Berlin Heidelberg; 2001.
2. Albrektsson TO, Johansson CB, Sennerby L. Biological aspects of implant dentistry: osseointegration. *Periodontology*. 2000;1994(4): 58-73.
3. Kwakman PHS, Zaat SAJ. In: Moriarty TF, Zaat SAJ, Busscher HJ, eds. *Biomaterials Associated Infection: Immunological Aspects and Antimicrobial Strategies*. Springer New York; 2013.
4. Lang NP, Wilson TG, Corbet EF. Biological complications with dental implants: their prevention, diagnosis and treatment. *Clin Oral Implants Res*. 2000;11:146-155.

5. Zimmerli W, Trampuz A. In: Moriarty TF, Zaat SAJ, Busscher HJ, eds. *Biomaterials Associated Infection: Immunological Aspects and Antimicrobial Strategies*. Springer New York; 2013.
6. Abdallah M-N, Badran Z, Ciobanu O, Hamdan N, Tamimi F. Strategies for optimizing the soft tissue seal around Osseointegrated implants. *Adv Healthc Mater*. 2017;6:1700549.
7. Guo T, Gulati K, Arora H, Han P, Fournier B, Ivanovski S. Orchestrating soft tissue integration at the transmucosal region of titanium implants. *Acta Biomater*. 2021;124:33-49.
8. Franz S, Rammelt S, Scharnweber D, Simon JC. Immune responses to implants – a review of the implications for the design of immunomodulatory biomaterials. *Biomaterials*. 2011;32:6692-6709.
9. Stanford CM. Surface modification of biomedical and dental implants and the processes of inflammation, wound healing and bone formation. *Int J Mol Sci*. 2010;11:354-369.
10. Meyers SR, Grinstaff MW. Biocompatible and bioactive surface modifications for prolonged in vivo efficacy. *Chem Rev*. 2012;112:1615-1632.
11. Han X, Shen T, Lou H. Dietary polyphenols and their biological significance. *Int J Mol Sci*. 2007;8:950-988.
12. Frei B, Higdon JV. Antioxidant activity of tea polyphenols in vivo: evidence from animal studies. *J Nutr*. 2003;133:3275S-3284S.
13. Zhang H, Tsao R. Dietary polyphenols, oxidative stress and antioxidant and anti-inflammatory effects. *Curr Opin Food Sci*. 2016;8:33-42.
14. Rahman I, Biswas SK, Kirkham PA. Regulation of inflammation and redox signaling by dietary polyphenols. *Biochem Pharmacol*. 2006;72:1439-1452.
15. Zhang H, Wu X, Wang G, et al. Macrophage polarization, inflammatory signaling, and NF- κ B activation in response to chemically modified titanium surfaces. *Colloids and Surf B*. 2018;166:269-276.
16. Lagha AB, Grenier D. Tea polyphenols protect gingival keratinocytes against TNF- α -induced tight junction barrier dysfunction and attenuate the inflammatory response of monocytes/macrophages. *Cytokine*. 2019;115:64-75.
17. Pan M-H, Lin-Shiau S-Y, Ho C-T, Lin J-H, Lin J-K. Suppression of lipopolysaccharide-induced nuclear factor- κ B activity by theaflavin-3,3'-digallate from black tea and other polyphenols through down-regulation of I κ B kinase activity in macrophages. *Biochem Pharmacol*. 2000;59:357-367.
18. Bodet C, Chandad F, Grenier D. Cranberry components inhibit interleukin-6, interleukin-8, and prostaglandin E2 production by lipopolysaccharide-activated gingival fibroblasts. *Eur J Oral Sci*. 2007;115:64-70.
19. Palaska I, Papathanasiou E, Theoharides TC. Use of polyphenols in periodontal inflammation. *Eur J Pharmacol*. 2013;720:77-83.
20. Bunte K, Hensel A, Beikler T. Polyphenols in the prevention and treatment of periodontal disease: a systematic review of in vivo, ex vivo and in vitro studies. *Fitoterapia*. 2019;132:30-39.
21. Barrett DG, Sileika TS, Messersmith PB. Molecular diversity in phenolic and polyphenolic precursors of tannin-inspired nanocoatings. *Chem Commun*. 2014;50:7265-7268.
22. Steffi C, Shi Z, Kong CH, Wang W. Bioinspired polydopamine and polyphenol tannic acid functionalized titanium suppress osteoclast differentiation: a facile and efficient strategy to regulate osteoclast activity at bone-implant interface. *J R Soc Interface*. 2019;16:20180799.
23. He R, Hu X, Tan HC, et al. Surface modification of titanium with curcumin: a promising strategy to combat fibrous encapsulation. *J Mater Chem B*. 2015;3:2137-2146.
24. Córdoba A, Satué M, Gómez-Florit M, et al. Flavonoid-modified surfaces: multifunctional bioactive biomaterials with Osteopromotive, anti-inflammatory, and anti-fibrotic potential. *Adv Healthc Mater*. 2015;4:540-549.
25. Geißler S, Gomez-Florit M, Wiedmer D, Barrantes A, Petersen FC, Tiainen H. In Vitro Performance of Bioinspired Phenolic Nanocoatings for Endosseous Implant Applications. *ACS Biomater Sci Eng*. 2019;5:3340.
26. Lee S, Chang Y-Y, Lee J, et al. Surface engineering of titanium alloy using metal-polyphenol network coating with magnesium ions for improved osseointegration. *Biomater Sci*. 2020;8:3404-3417.
27. Weber F, Liao W-C, Barrantes A, Edén M, Tiainen H. Silicate-phenolic networks: coordination-mediated deposition of bioinspired tannic acid coatings. *Chem A Eur J*. 2019;25:9870-9874.
28. Geißler S, Barrantes A, Tengvall P, Messersmith PB, Tiainen H. Deposition kinetics of bioinspired phenolic coatings on titanium surfaces. *Langmuir*. 2016;32:8050-8060.
29. Bergseth G, Ludviksen JK, Kirschfink M, Giclas PC, Nilsson B, Mollnes TE. An international serum standard for application in assays to detect human complement activation products. *Mol Immunol*. 2013;56:232-239.
30. Re R, Pellegrini N, Proteggente A, Pannala A, Yang M, Rice-Evans C. Antioxidant activity applying an improved ABTS radical cation decolorization assay. *Free Radic Biol Med*. 1999;26:1231-1237.
31. Graham HD. Stabilization of the Prussian blue color in the determination of polyphenols. *J Agric Food Chem*. 1992;40:801-805.
32. Boraldi F, Annovi G, Paolinelli-Devincenzi C, Tiozzo R, Quagliano D. The effect of serum withdrawal on the protein profile of quiescent human dermal fibroblasts in primary cell culture. *Proteomics*. 2008;8:66-82.
33. Vroman L, Adams AL. Findings with the recording ellipsometer suggesting rapid exchange of specific plasma proteins at liquid/solid interfaces. *Surf Sci*. 1969;16:438-446.
34. Vroman L, Adams AL, Fischer GC, Munoz PC. Interaction of high molecular weight kininogen, factor XII, and fibrinogen in plasma at interfaces. *Blood*. 1980;55:156-159.
35. Oćwieja M, Adamczyk Z, Morga M. Adsorption of tannic acid on polyelectrolyte monolayers determined in situ by streaming potential measurements. *J Colloid Interface Sci*. 2015;438:249-258.
36. You F, Xu Y, Yang X, Zhang Y, Shao L. Bio-inspired Ni²⁺-polyphenol hydrophilic network to achieve unconventional high-flux nanofiltration membranes for environmental remediation. *Chem Commun*. 2017;53:6128-6131.
37. Green RJ, Davies MC, Roberts CJ, Tendler SJB. Competitive protein adsorption as observed by surface plasmon resonance. *Biomaterials*. 1999;20:385-391.
38. Kubiak-Ossowska K, Tokarczyk K, Jachimska B, Mulheran PA. Bovine serum albumin adsorption at a silica surface explored by simulation and experiment. *J Phys Chem B*. 2017;121:3975-3986.
39. Fabre H, Mercier D, Galtayries A, Portet D, Delorme N, Bardeau J-F. Impact of hydrophilic and hydrophobic functionalization of flat TiO₂/Ti surfaces on proteins adsorption. *Appl Surf Sci*. 2018;432:15-21.
40. Roach P, Farrar D, Perry CC. Interpretation of protein adsorption: surface-induced conformational changes. *J Am Chem Soc*. 2005;127:8168-8173.
41. Chapin JC, Hajjar KA. Fibrinolysis and the control of blood coagulation. *Blood Rev*. 2015;29:17-24.
42. Sivaraman B, Latour RA. The relationship between platelet adhesion on surfaces and the structure versus the amount of adsorbed fibrinogen. *Biomaterials*. 2010;31:832-839.
43. Yang L, Han L, Liu Q, Xu Y, Jia L. Galloyl groups-regulated fibrinogen conformation: understanding antiplatelet adhesion on tannic acid coating. *Acta Biomater*. 2017;64:187-199.
44. Tardy BL, Richardson JJ, Nithipipat V, et al. Protein adsorption and coordination-based end-tethering of functional polymers on metal-phenolic network films. *Biomacromolecules*. 2019;20:1421-1428.
45. Diebolder CA, Beurskens FJ, de Jong RN, et al. Complement is activated by IgG hexamers assembled at the cell surface. *Science*. 2014;343:1260-1263.
46. Harmankaya N, Igawa K, Stenlund P, Palmquist A, Tengvall P. Healing of complement activating Ti implants compared with non-activating Ti in rat tibia. *Acta Biomater*. 2012;8:3532-3540.
47. Källtorp M, Askendal A, Thomsen P, Tengvall P. Inflammatory cell recruitment, distribution, and chemiluminescence response at IgG

- precoated- and thiol functionalized gold surfaces. *J Biomed Mater Res B*. 1999;47:251-259.
48. Deng L, Qi Y, Liu Z, Xi Y, Xue W. Effect of tannic acid on blood components and functions. *Colloids and Surf B*. 2019;184:110505.
 49. Wiegner R, Chakraborty S, Huber-Lang M. Complement-coagulation crosstalk on cellular and artificial surfaces. *Immunobiology*. 2016; 221:1073-1079.
 50. Merle NS, Church SE, Fremeaux-Bacchi V, Roumenina LT. Complement system part I – molecular mechanisms of activation and regulation. *Front Immunol*. 2015;6:262.
 51. Merle NS, Noe R, Halbwachs-Mecarelli L, Fremeaux-Bacchi V, Roumenina LT. Complement system part II: role in immunity. *Front Immunol*. 2015;6:6.
 52. Chenoweth DE. Complement activation in extracorporeal circuits. *Ann NY Acad Sci*. 1987;516:306-313.
 53. Andersson J, Ekdahl KN, Lambris JD, Nilsson B. Binding of C3 fragments on top of adsorbed plasma proteins during complement activation on a model biomaterial surface. *Biomaterials*. 2005;26: 1477-1485.
 54. Dahlbäck B. Blood coagulation. *Lancet*. 2000;355:1627-1632.
 55. Spronk HMH, Govers-Riemslog JWP, ten Cate H. The blood coagulation system as a molecular machine. *Bioessays*. 2003;25:1220-1228.
 56. Thor A, Rasmusson L, Wennerberg A, et al. The role of whole blood in thrombin generation in contact with various titanium surfaces. *Biomaterials*. 2007;28:966-974.
 57. Zhang G, Yang Y, Zhang T, et al. FeIII chelated organic anode with ultrahigh rate performance and ultra-long cycling stability for lithium-ion batteries. *Energy Storage Mater*. 2019;24:432-438.
 58. Sperling C, Fischer M, Maitz MF, Werner C. Blood coagulation on biomaterials requires the combination of distinct activation processes. *Biomaterials*. 2009;30:4447-4456.
 59. Sperling C, Maitz MF, Grasso S, Werner C, Kanse SM. A positively charged surface triggers coagulation activation through factor VII activating protease (FSAP). *ACS Appl Mater Interface*. 2017;9:40107-40116.
 60. Frost A, Jonsson KB, Ridefelt P, Nilsson O, Ljunghall S, Ljunggren Ö. Thrombin, but not bradykinin, stimulates proliferation in isolated human osteoblasts, via a mechanism not dependent on endogenous prostaglandin formation. *Acta Orthop Scand*. 1999;70:497-503.
 61. Thomas MR, Storey RF. The role of platelets in inflammation. *Thromb Haemost*. 2015;114:449-458.
 62. Eriksson O, Mohlin C, Nilsson B, Ekdahl KN. The human platelet as an innate immune cell: interactions between activated platelets and the complement system. *Front Immunol*. 2019;10:10.
 63. Choudhury A, Chung I, Blann AD, Lip GYH. Platelet Surface CD62P and CD63, Mean Platelet Volume, and Soluble/Platelet P-Selectin as Indexes of Platelet Function in Atrial Fibrillation. *J Am Coll Cardiol*. 1957;2007:49.
 64. Baggiolini M, Clark-Lewis I. Interleukin-8, a chemotactic and inflammatory cytokine. *FEBS Lett*. 1992;307:97-101.
 65. Kiss AK, Filipek A, Żyżyńska-Granica B, Naruszewicz M. Effects of Penta-O-galloyl-β-D-glucose on human neutrophil function: significant down-regulation of L-selectin expression. *Phytother Res*. 2013; 27:986-992.
 66. Weber F, Sagstuen E, Zhong Q-Z, Zheng T, Tiainen H. Tannic acid radicals in the presence of alkali metal salts and their impact on the formation of silicate-phenolic networks. *ACS Appl Mater Interface*. 2020;12:52457-52466.
 67. Lardner A. The effects of extracellular pH on immune function. *J Leukoc Biol*. 2001;69:522-530.
 68. Albrektsson T, Brånemark PI, Hansson H-A, et al. The interface zone of inorganic implants in vivo: titanium implants in bone. *Ann Biomed Eng*. 1983;11:1-27.
 69. Bainbridge P. Wound healing and the role of fibroblasts. *J Wound Care*. 2013;22:407-412.
 70. Michałowicz J, Duda W. Phenols – Sources and Toxicity. *Pol J Environ Stud*. 2007;16:347.
 71. Khan NS, Ahmad A, Hadi SM. Anti-oxidant, pro-oxidant properties of tannic acid and its binding to DNA. *Chem Biol Interact*. 2000;125: 177-189.
 72. Yen G-C, Duh P-D, Tsai H-L. Antioxidant and pro-oxidant properties of ascorbic acid and gallic acid. *Food Chem*. 2002;79:307-313.
 73. He D, Ma X, Chen Y, Cai Y, Ru X, Bruce IC, Xia Q, Shi G, Jin J. Luteolin inhibits pyrogallol-induced apoptosis through the extracellular signal-regulated kinase signaling pathway. *FEBS Journal*. 2012; 279:1834.
 74. Smith MT. Quinones as mutagens, carcinogens, and anticancer agents: introduction and overview. *J Toxicol Environ Health*. 1985; 16:665-672.
 75. Patrinely A, Clifford MN, Ioannides C. Contribution of phenols, quinones and reactive oxygen species to the mutagenicity of white grape juice in the Ames test. *Food Chem Toxicol*. 1996;34:869-872.
 76. Kern M, Fridrich D, Reichert J, et al. Limited stability in cell culture medium and hydrogen peroxide formation affect the growth inhibitory properties of delphinidin and its degradation product gallic acid. *Mol Nutr Food Res*. 2007;51:1163-1172.
 77. Hoffmann MH, Griffiths HR. The dual role of reactive oxygen species in autoimmune and inflammatory diseases: evidence from pre-clinical models. *Free Radic Biol Med*. 2018;125:62-71.
 78. Li X, Wang X, Zheng M, Luan QX. Mitochondrial reactive oxygen species mediate the lipopolysaccharide-induced pro-inflammatory response in human gingival fibroblasts. *Exp Cell Res*. 2016;347: 212-221.
 79. Meier B, Radeke HH, Selle S, et al. Human fibroblasts release reactive oxygen species in response to interleukin-1 or tumour necrosis factor-α. *Biochem J*. 1989;263:539-545.
 80. Cheng R, Choudhury D, Liu C, Billet S, Hu T, Bhowmick NA. Gingival fibroblasts resist apoptosis in response to oxidative stress in a model of periodontal diseases. *Cell Death Discov*. 2015;1:15046.
 81. Forman HJ, Torres M. Reactive oxygen species and cell signaling. *J Respir Crit Care Med*. 2002;166:54-58.
 82. Henderson LM, Chappell JB. Dihydrorhodamine 123: a fluorescent probe for superoxide generation? *Eur J Biochem*. 1993;217:973-980.
 83. Forrest VJ, Kang Y-H, McClain DE, Robinson DH, Ramakrishnan N. Oxidative stress-induced apoptosis prevented by trolox. *Free Radic Biol Med*. 1994;16:675-684.
 84. Yang Z, Tu Y, Xia H, Jie G, Chen X, He P. Suppression of free-radicals and protection against H₂O₂-induced oxidative damage in HPF-1 cell by oxidized phenolic compounds present in black tea. *Food Chem*. 2007;105:1349-1356.
 85. Riedl KM, Carando S, Alessio HM, McCarthy M, Hagerman AE. Antioxidant Activity of Tannins and Tannin-Protein Complexes: Assessment In Vitro and In Vivo. *Free Radicals in Food*. 2002;14. American Chemical Society.
 86. Ishii T, Mori T, Tanaka T, et al. Covalent modification of proteins by green tea polyphenol (–)-epigallocatechin-3-gallate through autooxidation. *Free Radic Biol Med*. 2008;45:1384-1394.
 87. Steffen MJ, Holt SC, Ebersole JL. *Porphyromonas gingivalis* induction of mediator and cytokine secretion by human gingival fibroblasts. *Oral Microbiol Immunol*. 2000;15:172-180.
 88. Agarwal S, Baran C, Piesco NP, et al. Synthesis of proinflammatory cytokines by human gingival fibroblasts in response to lipopolysaccharides and interleukin-1β. *J Periodontol Res*. 1995;30:382-389.
 89. Sivanantham A, Pattarayan D, Rajasekar N, et al. Tannic acid prevents macrophage-induced pro-fibrotic response in lung epithelial cells via suppressing TLR4-mediated macrophage polarization. *Inflammation Research*. 2019;68:1011-1024.

90. Aharoni S, Lati Y, Aviram M, Fuhrman B. Pomegranate juice polyphenols induce a phenotypic switch in macrophage polarization favoring a M2 anti-inflammatory state. *Biofactors*. 2015;41:44-51.
91. Nicolis E, Lampronti I, Dececchi MC, et al. Pyrogallol, an active compound from the medicinal plant *Emblica officinalis*, regulates expression of pro-inflammatory genes in bronchial epithelial cells. *Int Immunopharmacol*. 2008;8:1672-1680.
92. Xiong G, Ji W, Wang F, et al. Quercetin inhibits inflammatory response induced by LPS from *Porphyromonas gingivalis* in human gingival fibroblasts via suppressing NF- κ B signaling pathway. *Biomed Res Int*. 2019;2019:6282635.
93. Gutiérrez-Venegas G, Jiménez-Estrada M, Maldonado S. The effect of flavonoids on transduction mechanisms in lipopolysaccharide-treated human gingival fibroblasts. *Int Immunopharmacol*. 2007;7:1199-1210.
94. Gómez-Florit M, Monjo M, Ramis JM. Quercitrin for periodontal regeneration: effects on human gingival fibroblasts and mesenchymal stem cells. *Sci Rep*. 2015;5:16593.
95. Wheeler DS, Catravas JD, Odoms K, Denenberg A, Malhotra V, Wong HR. Epigallocatechin-3-gallate, a Green tea-derived polyphenol, inhibits IL-1 β -dependent Proinflammatory signal transduction in cultured respiratory epithelial cells. *J Nutr*. 2004;134:1039-1044.
96. Grenier D, Chen H, Ben Lagha A, Fournier-Larente J, Morin M-P. Dual action of myricetin on *Porphyromonas gingivalis* and the inflammatory response of host cells: a promising therapeutic molecule for periodontal diseases. *PLoS One*. 2015;10:e0131758.
97. Jang S-E, Hyam SR, Jeong J-J, Han MJ, Kim D-H. Penta-O-galloyl- β -D-glucose ameliorates inflammation by inhibiting MyD88/NF- κ B and MyD88/MAPK signalling pathways. *Br J Pharmacol*. 2013;170:1078-1091.
98. Martindale JL, Holbrook NJ. Cellular response to oxidative stress: signaling for suicide and survival. *J Cell Physiol*. 2002;192:1-15.
99. Pålsson-McDermott EM, O'Neill LAJ. Signal transduction by the lipopolysaccharide receptor, toll-like receptor-4. *Immunology*. 2004;113:153-162.
100. Martin KE, García AJ. Macrophage phenotypes in tissue repair and the foreign body response: implications for biomaterial-based regenerative medicine strategies. *Acta Biomater*. 2021;133:4-16.

SUPPORTING INFORMATION

Additional supporting information may be found in the online version of the article at the publisher's website.

How to cite this article: Weber F, Quach HQ, Reiersen M, et al. Characterization of the foreign body response of titanium implants modified with polyphenolic coatings. *J Biomed Mater Res*. 2022;110(7):1341-1355. doi:10.1002/jbm.a.37377